

## Late Quaternary deposition and facies model for karstic Lake Estanya (North-eastern Spain)

MARIO MORELLÓN\*, BLAS VALERO-GARCÉS\*, FLAVIO ANSELMETTI†, DANIEL ARIZTEGUI‡, MICHAEL SCHNELLMANN§, ANA MORENO\*¶, PILAR MATA\*\*, MAITE RICO\* and JUAN PABLO CORELLA\*

\*Department of Environmental Processes and Global Change, Pyrenean Institute of Ecology (IPE) – CSIC, Campus de Aula Dei, Avda Montañana 1005, E-50059 Zaragoza, Spain (E-mail: mariomm@ipe.csic.es)

†EAWAG, Swiss Federal Institute of Aquatic Research, Ueberlandstrasse 133, CH-8600 Duebendorf, Switzerland

‡Section of Earth Sciences, University of Geneva, Rue des Maraîchers 13. CH-1205 Genève, Switzerland

§Geological Institute – Swiss Federal Institute of Technology, Zürich (ETH), Sonneggstrasse 5, CH-8092 Zürich, Switzerland

¶Limnological Research Center (LRC), Department of Geology and Geophysics, University of Minnesota, 220 Pillsbury Hall/310 Pillsbury Drive S.E., Minneapolis, MN 55455-0219, USA

\*\*Facultad de Ciencias del Mar y Ambientales, Universidad de Cádiz, Polígono Río San Pedro s/n, 11510 Puerto Real (Cádiz), Spain

Associate Editor: Stephen Lokier

### ABSTRACT

Lake Estanya is a small (19 ha), freshwater to brackish, monomictic lake formed by the coalescence of two karstic sinkholes with maximum water depths of 12 and 20 m, located in the Pre-Pyrenean Ranges (North-eastern Spain). The lake is hydrologically closed and the water balance is controlled mostly by groundwater input and evaporation. Three main modern depositional sub-environments can be recognized as: (i) a carbonate-producing 'littoral platform'; (ii) a steep 'talus' dominated by reworking of littoral sediments and mass-wasting processes; and (iii) an 'offshore, distal area', seasonally affected by anoxia with fine-grained, clastic sediment deposition. A seismic survey identified up to 15 m thick sedimentary infill comprising: (i) a 'basal unit', seismically transparent and restricted to the depocentres of both sub-basins; (ii) an 'intermediate unit' characterized by continuous high-amplitude reflections; and (iii) an 'upper unit' with strong parallel reflectors. Several mass-wasting deposits occur in both sub-basins. Five sediment cores were analysed using sedimentological, microscopic, geochemical and physical techniques. The chronological model for the sediment sequence is based on 17 accelerator mass spectrometry <sup>14</sup>C dates. Five depositional environments were characterized by their respective sedimentary facies associations. The depositional history of Lake Estanya during the last *ca* 21 kyr comprises five stages: (i) a brackish, shallow, calcite-producing lake during full glacial times (21 to 17.3 kyr BP); (ii) a saline, permanent, relatively deep lake during the late glacial (17.3 to 11.6 kyr BP); (iii) an ephemeral, saline lake and saline mudflat complex during the transition to the Holocene (11.6 to 9.4 kyr BP); (iv) a saline lake with gypsum-rich, laminated facies and abundant microbial mats punctuated by periods of more frequent flooding episodes and clastic-dominated deposition during the Holocene (9.4 to 0.8 kyr BP); and (v) a deep, freshwater to brackish lake with high clastic input during the last 800 years. Climate-driven hydrological fluctuations are the main internal control in the evolution of the lake during the last 21 kyr,

1 affecting water salinity, lake-level changes and water stratification. However,  
 2 external factors, such as karstic processes, clastic input and the occurrence of  
 3 mass-flows, are also significant. The facies model defined for Lake Estanya is  
 4 an essential tool for deciphering the main factors influencing lake deposition  
 5 and to evaluate the most suitable proxies for lake level, climate and  
 6 environmental reconstructions and it is applicable to modern karstic lakes  
 7 and to ancient lacustrine formations.

8  
 9 **Keywords** Iberian Peninsula, karstic lake, lacustrine depositional environ-  
 10 ments, Late Quaternary, mass flow, palaeohydrology, sedimentary facies,  
 11 seismic stratigraphy.

## 14 INTRODUCTION

15 Quaternary lacustrine systems have been studied  
 16 extensively in the last decades (Gierlowski-  
 17 Kordesch & Kelts, 1994, 2000; Cohen, 2003).  
 18 New depositional models have been described  
 19 for a number of lake types based on modern  
 20 systems and Quaternary basins: playa, ephemeral  
 21 and shallow saline lakes (Eugster & Hardie, 1978;  
 22 Hardie *et al.*, 1978; Eugster & Kelts, 1983; Last,  
 23 1990; Smoot & Lowenstein, 1991; Renault & Last,  
 24 1994; Schreiber & Tabakh, 2000), carbonate-rich  
 25 lakes (Platt & Wright, 1991), volcanic-related  
 26 lakes (Negendank & Zolitschka, 1993; Nelson  
 27 *et al.*, 1994), tectonic basins (Lambiase, 1990),  
 28 glacial (Jopling, 1975) and fluvial lakes (Bohacks  
 29 *et al.*, 2000). Several projects coordinated by the  
 30 International Continental Scientific Deep Drilling  
 31 Project have provided new seismic and core data  
 32 for large and deep lake basins [for example, Great  
 33 Salt Lake (Balch *et al.*, 2005); Titicaca, (Fritz  
 34 *et al.*, 2007); Malawi, (Brown *et al.*, 2007); and  
 35 Petzen Itza (Anselmetti *et al.*, 2006; Hodell *et al.*,  
 36 2008)].

37  
 38 Considerably less attention has been paid to  
 39 perennial, freshwater, karstic lake systems  
 40 formed by solution of the sub-surface carbonate  
 41 or evaporite formations. Although the total area of  
 42 lakes formed by these processes is less than 1%  
 43 of total global lake area (Cohen, 2003) and most of  
 44 them are small, karstic lake basins are numerous  
 45 in regions such as temperate areas of Southern  
 46 China, North and Central America (Florida and  
 47 Yucatán) and the Mediterranean Basin (Spain,  
 48 Balkans), where carbonate or evaporite lithologies  
 49 are dominant.

50 These karstic depressions are generated by  
 51 dissolution processes, often involving sub-  
 52 sidence and/or collapse, thus leading to the  
 53 generation of funnel-shaped dolines with steep  
 54 margins, which generally are very deep for their  
 55 size (Palmquist, 1979; Cvijic, 1981; Gutiérrez-

Elorza, 2001; Gutiérrez *et al.*, 2008). This partic-  
 ular morphology, together with the frequent  
 interception of large aquifers, providing consid-  
 erable groundwater input, leads to the develop-  
 ment of relatively deep, perennial and frequently  
 seasonally or annually stratified lake systems,  
 even in semi-arid regions with negative hydro-  
 logical balances, for example, Lake Zoñar, South-  
 ern Spain (Valero-Garcés *et al.*, 2006);  
 Aguelmane Azigza, Atlas Mountains, Morocco  
 (Martin, 1981). Their development on evaporites  
 and carbonate substrates favours sulphate-rich  
 and carbonate-rich water chemical compositions  
 in the case of continental evaporitic bedrocks,  
 e.g. Lac de Besse, France (Nicod, 1999); Lake  
 Demiryurt gölü, Turkey (Alagöz, 1967); Laguna  
 Grande de Archidona, Spain (Pulido-Bosch,  
 1989); Lago de Banyoles, Spain (Julià, 1980),  
 and generally carbonate-rich and chloride-rich  
 compositions for lakes developed on marine  
 formations, e.g. Lake Vrana, Croatia (Schmidt  
*et al.*, 2000); Lake Zoñar, Spain (Valero-Garcés  
*et al.*, 2003).

The relatively small size of these topographically  
 closed basins and the connection to aquifers make  
 these systems very sensitive to regional hydrolog-  
 ical balances, experiencing considerable lake  
 level, water chemistry and biological fluctuations  
 in response to changes in effective moisture  
 (Cohen, 2003). In addition, the combination of  
 great depth with multiple episodes of karstification  
 in these endorheic basins can lead to thick deposits  
 with high sedimentation rates providing long,  
 continuous sedimentary sequences with high  
 temporal resolution, suitable for palaeohydrolog-  
 ical and palaeoclimate reconstructions [for  
 example, Lago d'Accesa, Italy (Magny *et al.*,  
 2006, 2007; Millet *et al.*, 2007); Lake Banyoles,  
 Spain (Perez-Obiol & Julià, 1994); Lago di  
 Pergusa, Italy (Sadori & Narcisi, 2001; Zanchetta  
*et al.*, 2007); Lake Zoñar, Spain (Valero-Garcés  
*et al.*, 2006; Martín-Puertas *et al.*, 2008)].

The sedimentary sequences from karstic lakes have been used previously for palaeoenvironmental and palaeoclimate analyses. To date, however, no detailed facies models have been defined. Compared with other lacustrine depositional environments (Kelts & Hsü, 1978; Dean, 1981; Dean & Fouch, 1983; Eugster & Kelts, 1983; Wright, 1990; Talbot & Allen, 1996), small karstic lakes show even more abrupt and complex lateral and vertical facies changes. This effect is because internal thresholds of some key factors (e.g. salinity and water chemistry, temperature, light penetration, oxygenation levels) are often modified by extreme events, such as floods (Moreno *et al.*, 2008; Valero Garces *et al.*, 2008) and mass-wasting processes (Bourrouilh-Le Jan *et al.*, 2007). To decipher the high-resolution palaeoenvironmental information archived in these lake sequences, depositional models are required to provide a dynamic framework for integrating all palaeolimnological data (Valero-Garcés & Kelts, 1995).

This paper presents a depositional facies model for small (19 ha) karstic Lake Estanya (North-eastern Spain) that could be applicable to similar modern and ancient sedimentary systems. Previous studies carried out in this lake basin (Wansard *et al.*, 1998; Riera *et al.*, 2004, 2006; Morellón *et al.*, 2008) have shown the potential of this site as a palaeoenvironmental archive but did not resolve the sedimentary evolution of the lake at a basin scale. The use of acoustic, seismic stratigraphy provides a quasi three-dimensional image of the sedimentary basin and direct evidence of major phases of lake-level changes and mass-wasting processes. A facies model has been defined, combining sedimentological features with their mineralogical and organic composition, and blended with the results of an extensive study of present-day depositional environments. Within the framework of this facies model, the relative importance of different factors influencing lake deposition for the last 21 000 years is investigated. Additionally, different proxies for reconstructing past hydrological changes in karstic systems are evaluated.

## REGIONAL SETTING

### Geological and geomorphological setting

'Balsas de Estanya' (42°02' N, 0°32' E; 670 m above sea-level) is a karstic lake complex located at the foothills of the Sierras Exteriores, the

External Pyrenean Ranges in Northern Spain (Martínez-Peña & Pocoví, 1984). The External Pyrenean Ranges are composed of Mesozoic formations with east–west trending folds and thrusts. Outcrops of Upper Triassic carbonate and evaporite formations along these structures have favoured karstification processes and the development of large poljes and dolines (IGME, 1982). The Balsas de Estanya lake complex is located in a relatively small endorheic basin of 2.45 km<sup>2</sup> (López-Vicente, 2007) (Fig. 1A and B) that belongs to a larger Miocene polje structure (Sancho-Marcén, 1988). An Upper Triassic low-permeability marl and claystone formation (Keuper facies) constitutes the lake basin substrate whereas Mid Triassic limestones and dolostone Muschelkalk facies outcrops make up the higher reliefs of the catchment (Sancho-Marcén, 1988). The karstic system consists of three dolines with water depths of 7 m, 20 m and one that is only seasonally flooded. Furthermore, a number of karstic depressions filled with Quaternary sediments also occur (IGME, 1982; Sancho-Marcén, 1988; López-Vicente, 2007).

### Climate and hydrogeology

The region has a Mediterranean continental climate characterized by a long summer drought (León-Llamazares, 1991). The mean annual temperature is 14 °C with monthly means ranging from 4 (January) to 24 °C (July). Mean annual rainfall is 470 mm whereas the mean annual evapotranspiration rate has been estimated as 774 mm (Meteorological Station at Santa Ana Reservoir, 17 km south-east of the lake). July is the driest month with an average rainfall of 18 mm and October is the most humid month (50 mm).

The main lake basin, 'Estanque Grande de Abajo' (42°02' N, 0°32' E, 670 m a. s. l.), is an uvala formed by the coalescence of two sub-basins with maximum water depths of 12 and 20 m and steep margins (Ávila *et al.*, 1984). These two sub-basins are separated by a sill, 2 to 3 m below the present-day lake level, which only emerges during prolonged dry periods, for example, during the 1994 to 1996 drought (Morellón *et al.*, 2008). The total lake surface is 188 306 m<sup>2</sup>, with a maximum length of 850 m and a maximum width of 340 m. Total volume has been estimated as 983 728 m<sup>3</sup> (Ávila *et al.*, 1984).

The 'Estanque Grande de Abajo' has a relatively small watershed [106.50 ha surface (López-Vicente, 2007)]. Although there is no permanent



COLOUR

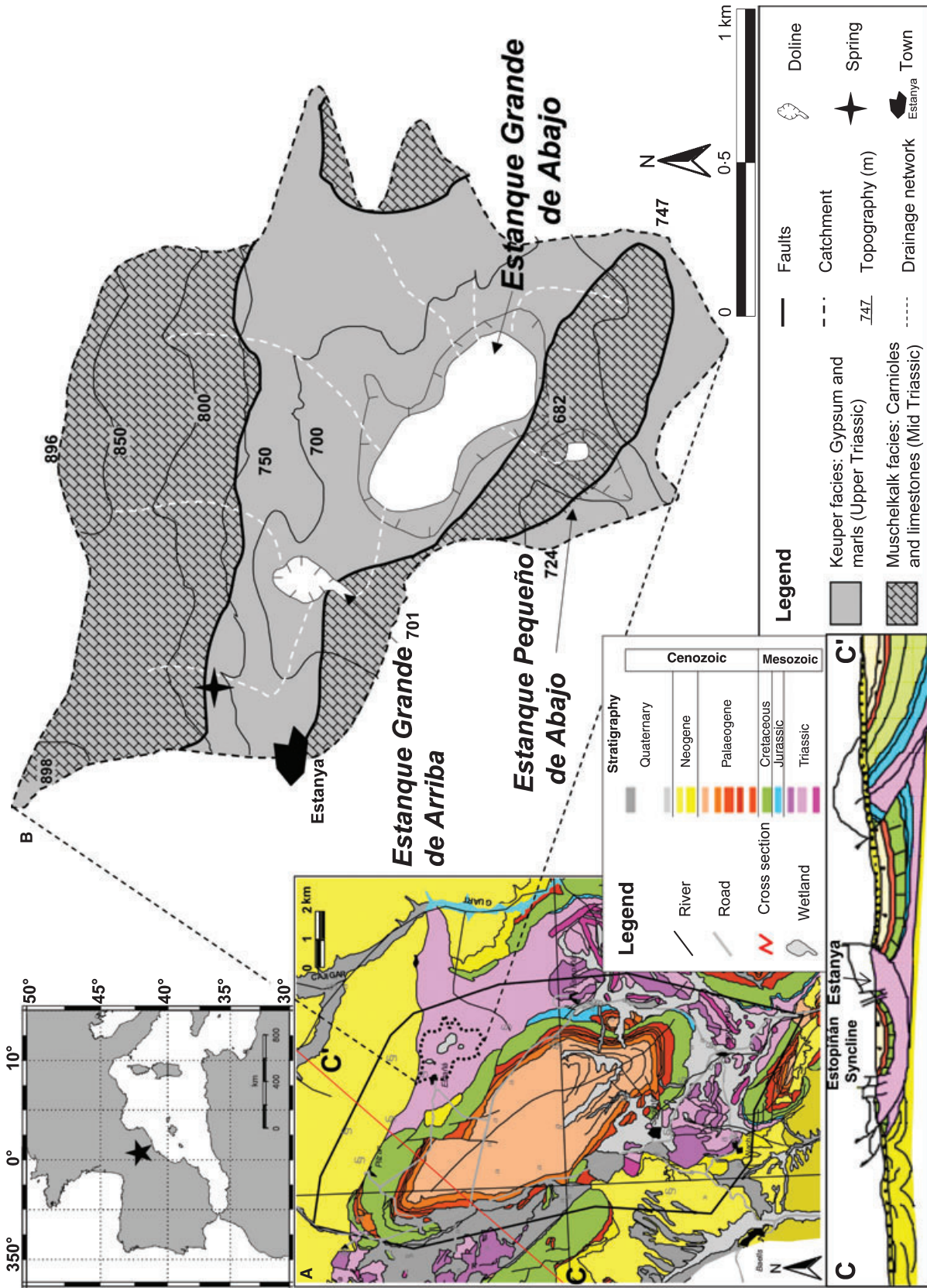


Fig. 1. Location map of Balsas de Estanya karstic lake system: (A) geological map and cross-section (C–C') of the Estopiñán Syncline (main hydrogeological system in the area) and surroundings (modified from Villa & Gracia, 2004); (B) topographic and geological map of Balsas de Estanya catchment (see legend below).

inlet, several ephemeral creeks drain the catchment providing clastic material to the lake during extreme precipitation events; alluvial and colluvial deposits occur in the northern and eastern littoral areas (López-Vicente, 2007). Archaeological evidence indicates that there has been water management in the area since the 12th century (Riera *et al.*, 2004, 2006). An artificial canal feeds the main lake when the water capacity of the small lake is exceeded. However, given the low water volume provided by this canal, it is discarded as a significant input to the lake.

There is no surface outlet and the nature of the substrate, composed of low permeability Upper Triassic Keuper facies, limits groundwater losses. Consequently, modern hydrology of Lake Estanya is controlled mostly by groundwater inputs and evaporation output. Calculated evapotranspiration exceeds rainfall by about 300 mm year<sup>-1</sup>. The lake is fed mainly by groundwaters from the surrounding local dolostone aquifer (Muschelkalk), probably related to the hydrogeological system of the Estopiñán Syncline (Villa & Gracia, 2004). A permanent spring (0.3 l sec<sup>-1</sup>) (Villa & Gracia, 2004) is located at the north end of the polje feeding the small Estanque Grande de Arriba (Fig. 1B). There are no available groundwater and lake level data to calculate the hydrological balance in the lake. However, the response of the system to precipitation is relatively rapid, as indicated by the observed *ca* 1 m lake-level drop during the relatively dry year 2005, and by the 2 to 3 m lake-level drop during the previous long dry period 1994 to 1996 when the central sill separating the two sub-basins emerged (Morellón *et al.*, 2008).

### Limnology

Lake water is brackish (electrical conductivity, 2,33200 μS cm<sup>-1</sup> and TDS, 3400 mg l<sup>-1</sup>), and sulphate and calcium-rich: [SO<sub>4</sub><sup>2-</sup>] > [Ca<sup>2+</sup>] > [Mg<sup>2+</sup>] > [Na<sup>+</sup>]. The lake is monomictic, with thermal stratification and anoxic hypolimnetic conditions during spring and summer, extending from March to September, and oligotrophic (Ávila *et al.*, 1984) (Table 1). Vertical profiling in September 2007 revealed thermal stratification with a thermocline located at 6 to 9 m water depth (Fig. 2, Table 1). The higher electrical conductivity in the epilimnion indicates the relative importance of evaporation loss. Differences in water chemistry with the nearby Estanya spring (Table 1) also suggest a long residence time and a high influence of evaporation on the system, as pointed out by

**Table 1.** Physical and chemical properties of the Estanya Spring and Lake Estanya (south-east sub-basin) at the lake surface and 16 m water depth for 24 June 2005 (summer stratification season).

| Sample         | Water depth (m) | Temperature (°C) | Conductivity (μS cm <sup>-1</sup> ) | pH   | Oxygen saturation (%) |      | Mg (mg l <sup>-1</sup> ) | K (mg l <sup>-1</sup> ) | Na (mg l <sup>-1</sup> ) | Sr (mg l <sup>-1</sup> ) | Li (mg l <sup>-1</sup> ) | Ca (mg l <sup>-1</sup> ) | HCO <sub>3</sub> (mg l <sup>-1</sup> ) | Cl (mg l <sup>-1</sup> ) | SO <sub>4</sub> (mg l <sup>-1</sup> ) |
|----------------|-----------------|------------------|-------------------------------------|------|-----------------------|------|--------------------------|-------------------------|--------------------------|--------------------------|--------------------------|--------------------------|--|--------------------------|---------------------------------------|
|                |                 |                  |                                     |      |                       |      |                          |                         |                          |                          |                          |                          |  |                          |                                       |
| Estanya Spring | -               | 14.0             | 627                                 | 7.64 | 100.0                 | 12.7 | 1.7                      | 20.5                    | 0.23                     | 0.11                     | 55.3                     | 0.3                      | 1.2                                    | 48.5                     |                                       |
| Lake Estanya   | 0               | 24.3             | 3 440                               | 7.63 | 65.8                  | 132  | 14.2                     | 133                     | 7.8                      | 0.16                     | 440                      | 1.37                     | 6.6                                    | 1813.1                   |                                       |
| Lake Estanya   | 16              | 5.1              | 3 330                               | 7.39 | 0.0                   | 127  | 14                       | 124                     | 7.1                      | 0.15                     | 402                      | 1.49                     | 6.3                                    | -                        |                                       |

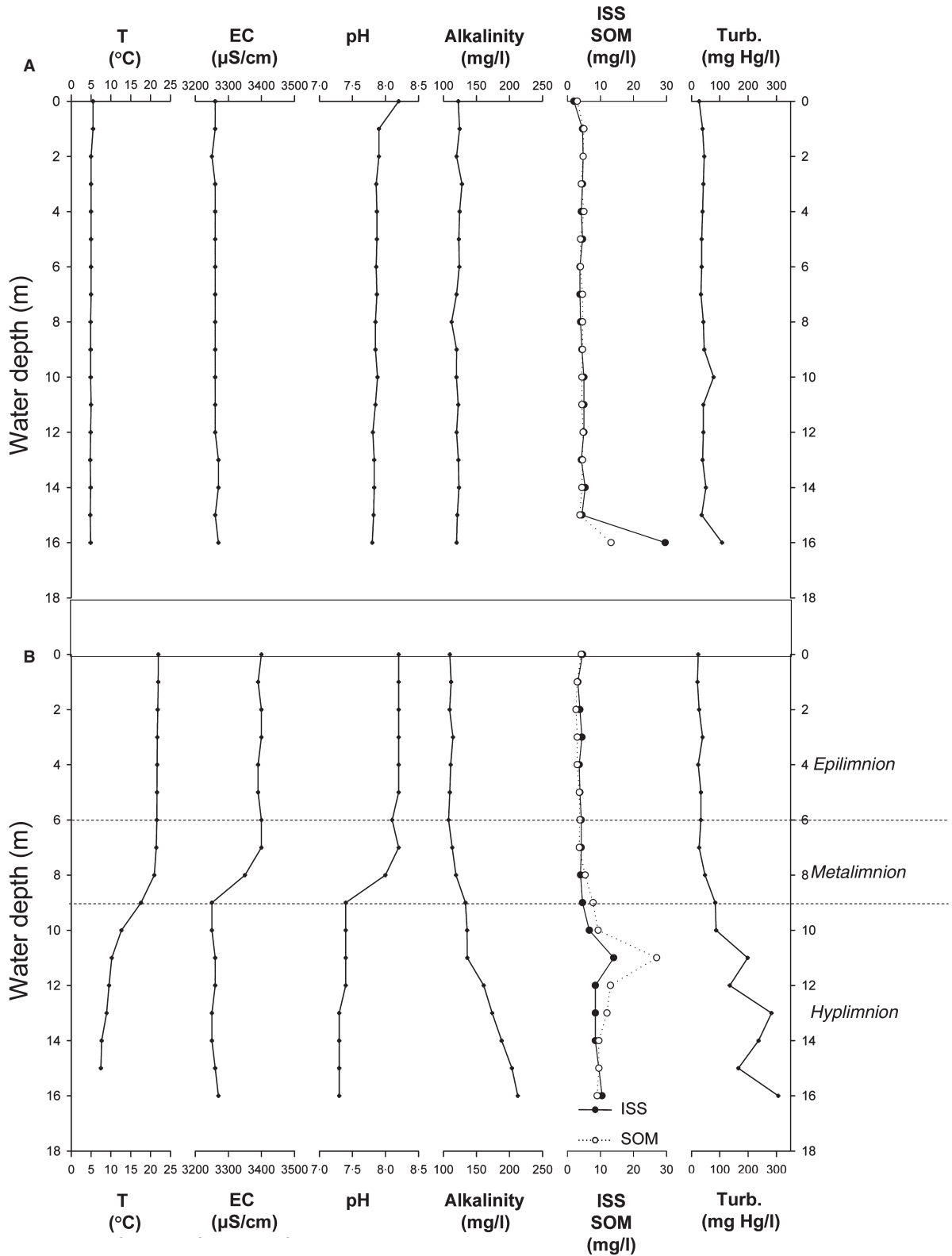


**Fig. 2.** Physical-chemical vertical profiles of the water column at the deepest area of *Estanque Grande de Abajo*. (A) Vertical profile measured in January 2008 (winter mixing period); (B) vertical profile measured in September 2007 (summer stratification period). From left to right: *T* ( $^{\circ}\text{C}$ ), temperature; EC ( $\mu\text{S cm}^{-1}$ ), electrical conductivity; pH; alkalinity ( $\text{mg l}^{-1}$ ); ISS ( $\text{mg l}^{-1}$ ), inorganic suspended solids; SOM ( $\text{mg l}^{-1}$ ), suspended organic matter; Turb. ( $\text{mgHg l}^{-1}$ ), turbidity.



1 previous studies (Villa & Gracia, 2004). An addi-  
 2 tional vertical profile measured in February 2008  
 3 revealed a well-mixed water column with homo-  
 4 geneous thermal and oxic conditions throughout  
 5 (Fig. 2A). Suspended solids are higher during the  
 6 summer season (Fig. 2B) revealing an important  
 7 contribution of clastic material derived from the  
 8 erosion of soils after the harvest (López-Vicente  
 9 *et al.*, 2008). Anoxic hypolimnetic conditions  
 10 during the summer stratification period favour  
 11 organic matter (OM) preservation, as indicated by  
 12 the increase in the relative amount of suspended  
 13 OM in respect to the inorganic suspended sedi-  
 14 ments below 9 m water depth (Fig. 2B). Sulphide  
 15 precipitation is favoured by the activity of sul-  
 16 phate-reducing bacteria (SRB) in the hypolimnion  
 17 (Esteve *et al.*, 1983; Guerrero *et al.*, 1987; Mir-  
 18 Puyuelo, 1997; Ramírez-Moreno, 2003). Maxi-  
 19 mum alkalinity values in the epilimnion are  
 20 reached in the summer season, coinciding with  
 21 the maximum algal productivity (Fig. 2B). During  
 22 this season, alkalinity increases with increasing  
 23 water depth, as a result of dissolution of carbon-  
 24 ates at the hypolimnion, where pH is lowered by  
 25 SRB-derived sulphide input (Ávila *et al.*, 1984).

## 28 MATERIALS AND METHODS

29 The Lake Estanya watershed was identified and  
 30 mapped using topographic and geological maps  
 31 and aerial photographs. Both lake sub-basins  
 32 were geophysically surveyed in June 2002 using  
 33 a high-resolution, single-channel seismic system  
 34 with a centre frequency of 3.5 kHz (GeoAcoustic  
 35 pinger source) of the ETH-Zürich (Zürich, Swit-  
 36 zerland). The source/receiver was mounted on a  
 37 catamaran raft that was pushed by a boat. The  
 38 studied basins were covered with a dense grid of  
 39 *ca* 6 km of seismic lines providing a mean spatial  
 40 resolution of *ca* 50 m between each line. Seismic-  
 41 processing workshop software was used for pro-  
 42 cessing of the data (bandpass filter, water bottom  
 43 mute) and the resulting seismic data set was  
 44 4 interpreted using the KINGDOM SUITE software.

45 Surface sediments were sampled with a  
 46 Uwitec<sup>®</sup> short-corer (Uwitec, Mondsee, Austria)  
 47 at 34 selected points distributed in a grid covering  
 48 all present-day depositional environments. The  
 49 uppermost 1 cm of each short core was sampled  
 50 and sediment aliquots were sub-sampled for  
 51 different analyses. Grain-size was determined  
 52 using a Coulter particle-size analyser (Beckman  
 53 Coulter Inc, Fullerton, CA, USA) (Buurman *et al.*,  
 54 1997). Samples were treated with 10% hydrogen

peroxide in a water bath at 80 °C to eliminate the  
 OM; a dispersant agent and ultrasound treatment  
 were used prior to measurement. Total organic  
 carbon (TOC) and total inorganic carbon (TIC)  
 were measured with a LECO SC 144 DR elemental  
 analyser (LECO Corporation, St Joseph, MI, USA)  
 and total nitrogen (TN) with a VARIOMAX CN  
 (Elementar Analysensysteme GMBH, Hanau,  
 Germany). Whole sediment mineralogy was  
 characterized by X-ray diffraction with a Philips  
 PW1820 diffractometer (Philips Analytical,  
 PANalytical B.V., Almelo, the Netherlands)  
 and relative mineral abundance was determined  
 using peak intensity following the procedures  
 described in Chung (1974a,b). Mapping of  
 different sediment properties through the lake  
 floor was carried out with ARCMAP 9.0<sup>®</sup>, using the  
 inverse distance weighted (IDW) interpolation  
 tool.

Coring operations were conducted in two  
 phases: four cores were retrieved in 2004 using  
 modified Kullenberg piston coring equipment  
 and platform from the Limnological Research  
 Center (LRC) (University of Minnesota, Minnea-  
 polis, MN, USA) and an additional Uwitec<sup>®</sup>  
 piston core (Uwitec) was recovered in 2006. The  
 longest cores (1A-1K and 5A-1U) reached 4.5 and  
 11 m below the lake floor, respectively.

Physical properties (magnetic susceptibility  
 and density) were measured in all cores with a  
 Geotek Multi-Sensor Core Logger (MSCL; Geotek  
 Limited, Daventry, UK) every 1 cm. The cores  
 were subsequently split in two halves and imaged  
 with a DMT Core Scanner (DMT GmbH & Co KG,  
 Essen, Germany) and a GEOSCAN II digital  
 camera (Geotek Limited). Sedimentary facies  
 were defined after visual, microscopic observa-  
 tion of smear slides in both superficial sediment  
 and in the core samples, following the method-  
 ology described in (Schnurrenberger *et al.*, 2003).

Cores were sub-sampled every 2 cm for TOC  
 and TIC and every 5 cm for mineralogical analy-  
 ses following the methodology described above.  
 Scanning electron microscope images were taken  
 under low-vacuum conditions in an environmen-  
 tal scanning electron microscope on uncoated  
 fragment samples. Backscattered electron images  
 were obtained to see compositional differences of  
 the components as grey-level contrast. Images  
 reflect the average chemical composition of grains  
 with the darker grains being made-up of lighter  
 elements than the brighter grains. In addition,  
 energy dispersive X-ray spectrometric analysis  
 (Phoenix system; EDAX, Mahwah, NJ, USA) was  
 performed when necessary.

The chronology for the lake sequence is constrained by 17 accelerator mass spectrometry (AMS)  $^{14}\text{C}$  dates analysed at the Poznan Radiocarbon Laboratory (Poland) (Tables 2 and 3). Although most of the dated samples correspond to terrestrial macro-remains, in eight samples bulk OM was analysed because of the absence of organic rests. The reservoir effect was calculated after dating pairs of bulk OM samples and terrestrial organic macrorests at three depth intervals representative of different sediment compositions and time-periods (Table 2). The correction was applied to dates not derived from macrorests. Corrected radiocarbon dates were

calibrated using CALPAL\_A software and the INTCAL04 curve (Riera *et al.*, 2004), selecting the median of the 95.4% distribution ( $2\sigma$  probability interval). The age–depth relationship was estimated by means of a generalized mixed-effect regression (Heegaard *et al.*, 2005).

## RESULTS

### Seismic stratigraphy

Seismic penetration into the sub-surface down to the acoustic basement allowed tracking of the

**Table 2.** Comparison between pairs of radiocarbon dates obtained after analyzing bulk organic sediment and plant macro-remains at the same core depth intervals.

| Core | Comp. depth (cm) | Laboratory code | Type of material       | $^{14}\text{C}$ AMS age (yr BP) | Calculated reservoir effect ( $^{14}\text{C}$ years) |
|------|------------------|-----------------|------------------------|---------------------------------|--|
| 1A   | 35.5             | Poz-24749       | <i>Phragmites</i> stem | 155 ± 30                        |  |
|      |                  | Poz-24760       | Bulk organic matter    | 740 ± 30                        | 585 ± 60   |
|      | 439.5            | Poz-9891        | Wood fragment          | 8510 ± 50                       |  |
|      |                  | Poz-23670       | Bulk organic matter    | 9330 ± 50                       | 820 ± 100  |
| 5A   | 890.6            | Poz-17194       | Wood fragment          | 16100 ± 80                      | Reworked   |
|      |                  | Poz-23671       | Bulk organic matter    | 15160 ± 90                      | –*   |

The calculated reservoir effect is indicated for each of the bulk organic matter samples.

\*The negative reservoir effect obtained in this sample ( $-940 \pm 170$ ) is because of the reworked nature of the terrestrial organic macrorest.

**Table 3.** Radiocarbon dates used for the construction of the age model for the Lake Estanya sequence. A correction of  $820 \pm 100$   $^{14}\text{C}$  years was applied to bulk sediment samples from Units II to VI. Corrected dates were calibrated using CALPAL\_A software and the INTCAL04 curve (Riera *et al.*, 2004); and the mid-point of 95.4% ( $2\sigma$  probability interval) was selected.

| Comp. depth (cm) | Laboratory code | Type of material                | AMS $^{14}\text{C}$ age (yr BP) | Corrected AMS $^{14}\text{C}$ age (yr BP) | Calibrated age (cal yr BP) (range $2\sigma$ ) |
|------------------|-----------------|---------------------------------|---------------------------------|---|---|
| Core 1A          |                 |                                 |                                 |   |   |
| 35.5             | Poz-24749       | <i>Phragmites</i> stem fragment | 155 ± 30                        | 155 ± 30                                  | 160 ± 100                                     |
| 61.5             | Poz-12245       | Plant remains and charcoal      | 405 ± 30                        | 405 ± 30                                  | 460 ± 60                                      |
| 177              | Poz-12246       | Plant remains                   | 895 ± 35                        | 895 ± 35                                  | 840 ± 60                                      |
| 196.5            | Poz-15972       | Bulk organic matter             | 2120 ± 30                       | 1300 ± 130                                | 1210 ± 130                                    |
| 240              | Poz-12247       | <i>Salix</i> leave              | 3315 ± 35                       | 3315 ± 35                                 | 3550 ± 50                                     |
| 337.5            | Poz-12248       | <i>Graminea</i> seed            | 5310 ± 60                       | 5310 ± 60                                 | 6100 ± 90                                     |
| 350              | Poz-15973       | Bulk organic matter             | 6230 ± 40                       | 5410 ± 140                                | 6180 ± 150                                    |
| 390              | Poz-15974       | Bulk organic matter             | 8550 ± 50                       | 7730 ± 150                                | 8600 ± 180                                    |
| 439.5            | Poz-9891        | Wood fragment                   | 8510 ± 50                       | 8510 ± 50                                 | 9510 ± 30                                     |
| Core 5A          |                 |                                 |                                 |   |   |
| 478.6            | Poz-17190       | Plant macroremain               | 8830 ± 50                       | 8830 ± 50                                 | 9940 ± 150                                    |
| 549.6            | Poz-17191       | Bulk organic matter             | 10 680 ± 60                     | 9860 ± 160                                | 11 380 ± 270                                  |
| 614.6            | Poz-20138       | Bulk organic matter             | 11 820 ± 60                     | 11 000 ± 160                              | 12 980 ± 120                                  |
| 659.6            | Poz-17192       | Macroremain                     | 11 710 ± 60                     | 11 710 ± 60                               | 13 570 ± 90                                   |
| 680.1            | Poz-20139       | Bulk organic matter             | 12 700 ± 70                     | 11 880 ± 170                              | 13 730 ± 190                                  |
| 704.1            | Poz-20067       | Bulk organic matter             | 13 280 ± 60                     | 12 460 ± 160                              | 14 550 ± 300                                  |
| 767.6            | Poz-17283       | Bulk organic matter             | 14 830 ± 90                     | 14 010 ± 190                              | 16 730 ± 270                                  |
| 957.5            | Poz-20140       | Plant remains                   | 15 130 ± 100                    | 15 130 ± 100                              | 18 420 ± 220                                  |



1 bedrock morphology in most parts of the lake.  
 2 Sediment thickness reaches up to *ca* 15 m in both  
 3 sub-basins with two depocentres occurring at the  
 4 deepest areas. Seismic stratigraphic analysis  
 5 allowed the identification of three major seismic  
 6 units ('A' to 'C'; Fig. 3A) and several seismic  
 7 horizons, which have been tracked through the  
 8 basins. These horizons and units were correlated  
 9 with the core lithostratigraphy. A constant acoustic  
 10 velocity of 1500 m sec<sup>-1</sup> based on the MSCL  
 11 measurements has been used for the seismic-to-  
 12 core correlation (Fig. 3A).

13 The bedrock surface is locally irregular and  
 14 marked by discrete steps and sharp edges, prob-  
 15 ably reflecting the karstic origin of the two  
 16 depressions. Overlying the acoustic basement,  
 17 Seismic unit 'C' is characterized by low-ampli-  
 18 tude reflections that are mostly continuous, and  
 19 intercalated with seismically transparent units.  
 20 Based on this pattern, a rather homogeneous  
 21 sediment composition is assumed lacking major  
 22 impedance contrasts (Fig. 3A). Only few med-  
 23 ium-amplitude reflections occur towards the top  
 24 of the unit, coinciding with the density contrasts  
 25 caused by alternating gypsum-rich and clastic  
 26 lithologies. The thickness of seismic unit 'C' is  
 27 highly variable reaching up to 10 m towards the  
 28 depocentres of both sub-basins, whereas it is  
 29 nearly absent in proximal areas of the basin and  
 30 on the sill.

31 Seismic unit 'B' is characterized by closely  
 32 spaced high-amplitude reflections, increasing  
 33 upwards as a result of more frequent lithological  
 34 changes towards the top of the unit. Correlation  
 35 with core lithostratigraphy shows that the high  
 36 number of reflections corresponds to the physical  
 37 contrast between alternating gypsum beds (high  
 38 density) with organic-rich lithologies (low den-  
 39 sity) containing massive silts. Well-defined  
 40 parallel reflections are more common in distal  
 41 areas representing probably more clastic and finer  
 42 facies, whereas alternating parallel-to-chaotic  
 43 seismic facies are found in proximal areas, prob-  
 44 ably reflecting a more dynamic sedimentation  
 45 affected by truncation surfaces as a result of  
 46 alternating deposition and erosion cycles. The  
 47 general sediment geometry, characterized in  
 48 underlying unit 'C' by a ponding style, changes  
 49 in unit 'B' to a draping pattern, so that unit 'B'  
 50 covers most of the lake with a maximum thick-  
 51 ness of *ca* 4 m.

52 Seismic unit 'A' is characterized by varying  
 53 seismic facies ranging between low-amplitude  
 54 to high-amplitude reflections that are all later-  
 55 ally continuous. The corresponding lithologies

observed in the core comprise rather homogenous  
 clastic and fine-grained sediments with a few  
 thin intervals rich in plant debris and coarser-  
 grained centimetre-thick intercalations. The latter  
 are more frequent in the south-eastern sub-basin  
 explaining the higher amplitudes of seismic  
 reflections when compared with the north-  
 western sub-basin. Unit 'A' is also of a draping  
 geometry with a thickness of up to *ca* 3 m,  
 reaching far into the littoral areas of the lake.

The seismic survey identified several small  
 mass-wasting deposits, particularly in the south-  
 eastern sub-basin. The largest mass-wasting de-  
 posit is restricted to the north-eastern margin of  
 the south-eastern sub-basin, and has a character-  
 istic mound-shaped morphology, with an irregu-  
 lar lower surface, a slightly hummocky upper  
 surface and a lobe-shaped distal termination  
 (Fig. 3A). The internal structure is character-  
 ized by chaotic to transparent seismic facies, typical of  
 mass flows (Mitchum *et al.*, 1977; Coleman &  
 Prior, 1988; Schnellmann *et al.*, 2005). The max-  
 imum lateral extent of this deposit is *ca* 150 m  
 and its maximum thickness reaches *ca* 5 m.  
 Seismic-to-core correlation of the horizon picked  
 on the top of the mass-flow deposit shows that it  
 occurred around the transition between seismic  
 units 'A' and 'B' (*ca* 800 cal yr BP, according to the  
 age model in this study). Similar mass flow  
 deposits occur also within seismic unit 'C',  
 mostly in the north-western sub-basin (Fig. 3A).

The change in sedimentation style through time  
 reflects large changes in the lake system. The  
 thinning and onlapping of unit 'C' towards the  
 slopes and sill areas suggest that the two sub-  
 basins were not permanently connected during  
 the early stages of basin evolution. Although  
 sediment-focusing processes because of lateral  
 sediment transport may have contributed to this  
 sediment geometry, this pattern is more probably  
 a reflection of predominating isolation of both  
 sub-basins during this initial lake stage. In con-  
 trast, the rather constant thickness of units 'A'  
 and 'B' throughout the basin result in draping  
 geometries and wider lateral extent, as well as the  
 good lateral correlation of reflections between the  
 two sub-basins, indicate that they have been  
 predominantly connected during deposition of  
 those units. The deposition of unit 'A' is not only  
 laterally continuous throughout the lake basin but  
 shows a similar thickness in the littoral areas  
 pointing to a regular and stable sedimentation  
 over the entire lake area in recent times. The  
 limited lateral changes in seismic facies of unit  
 'A', however, can be related to the present-day

1  
2  
3  
4  
5  
6  
7  
8  
9  
10  
11  
12  
13  
14  
15  
16  
17  
18  
19  
20  
21  
22  
23  
24  
25  
26  
27  
28  
29  
30  
31  
32  
33  
34  
35  
36  
37  
38  
39  
40  
41  
42  
43  
44  
45  
46  
47  
48  
49  
50  
51  
52  
53  
54  
55

COLOUR

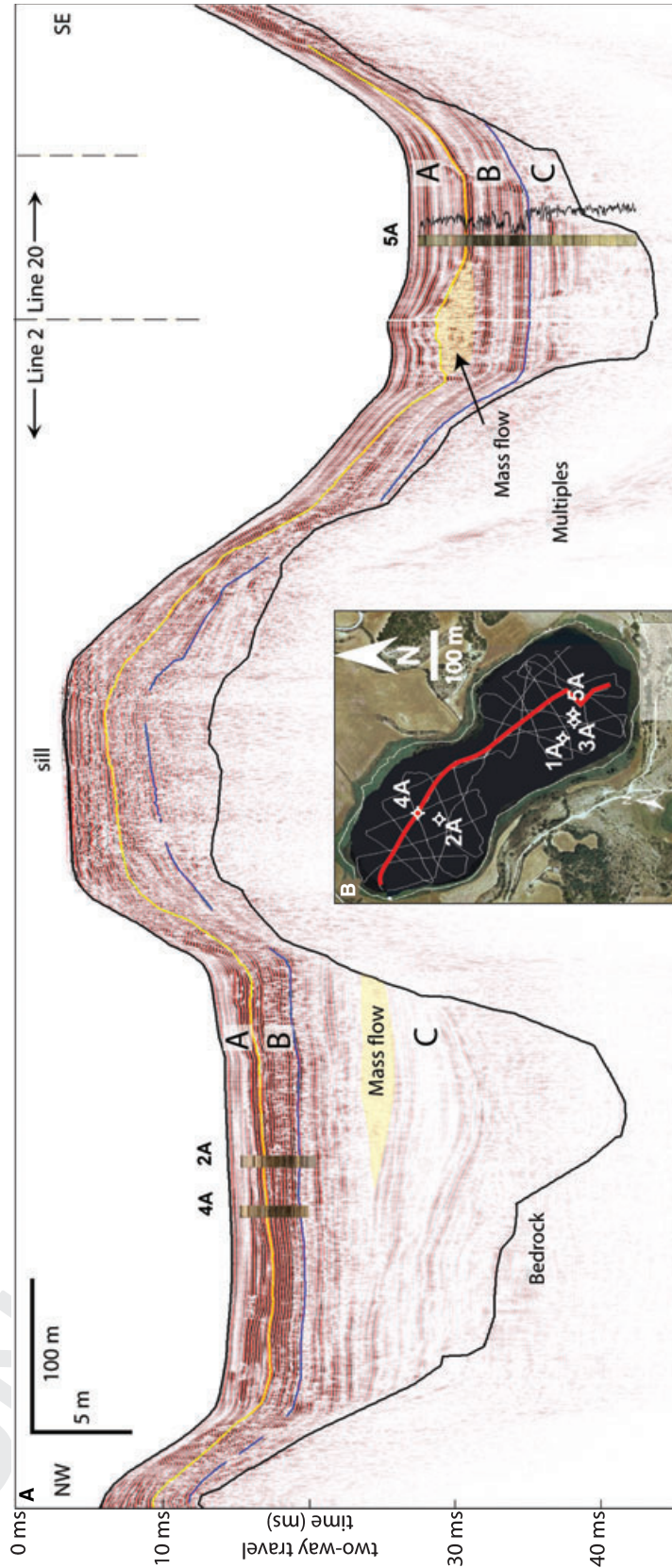


**Fig. 3.** (A) NW-SE seismic section (connected Line 2 and Line 20) crossing both sub-basins and the sill. Note the two kinks in the track marked by dashed lines on top. Three seismic units ('A' to 'C') can be identified in the sedimentary succession overlying the basement. Correlation with cores 2A, 4A and 5A is also indicated by superposition of core images and additionally density ( $\text{g cm}^{-3}$ ) profile for core 5A. (B) The inset map shows the seismic grid overlain on an aerial photograph with an indication of the long-core locations.

1 distribution of depositional sub-environments in  
 2 the lake basin (Fig. 3A).

3  
 4 **Sedimentary facies and depositional  
 5 environments**

6  
 7 *Present-day sedimentary facies and deposi-  
 8 tional sub-environments*

9 Sedimentary facies in modern Lake Estanya were  
 10 described and interpreted based on 34 sampling  
 11 points (Fig. 4). The relatively small size of the  
 12 lake, its topographically closed watershed and its  
 13 double funnel-shaped morphology (López-Vicente,  
 14 2007) determine the present low-energy deposi-  
 15 tional environments, relatively small lake-level  
 16 fluctuations (2 to 3 m) and the development of  
 17 seasonal anoxia in the deepest areas. The modern  
 18 lake could be described as a freshwater to brack-  
 19 ish, relatively deep, carbonate-producing, mono-  
 20 mictic lake, with some similarities to the  
 21 carbonate lake models described by Murphy &  
 22 Wilkinson (1980) and Platt & Wright (1991).  
 23 According to sedimentological features, grain-  
 24 size distribution, mineralogical content and OM  
 25 composition, three main depositional sub-envi-  
 26

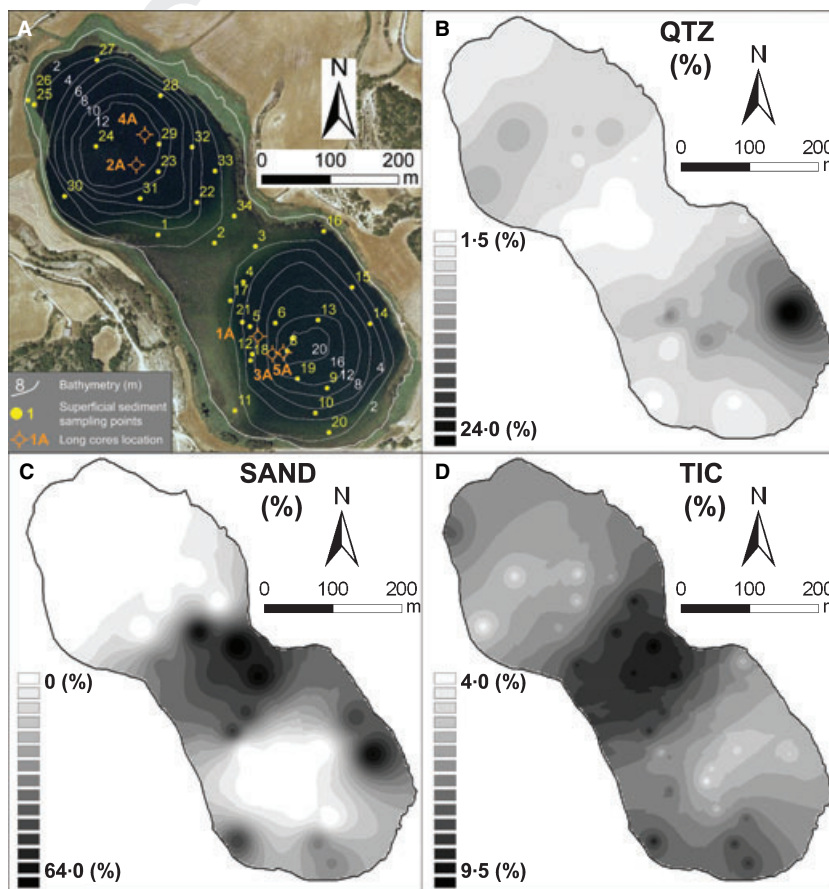
ronments can be identified in the modern lake  
 basin (Fig. 5A): (i) the littoral platform; (ii) the  
 transitional area; and (iii) the offshore, distal area.

(i) The ‘littoral platform’ constitutes a flat area,  
 partially colonized by vegetation that protects the  
 littoral zones from waves, stabilizes the substrate,  
 provides support for epiphytic fauna and largely  
 contributes to the production of carbonate partic-  
 les. This sub-environment is better developed  
 along the southern shores and in the sill, both  
 characterized by gentle slopes, and it is spatially  
 restricted to a narrow strip on the steep northern  
 shore (Fig. 5A).

The ‘internal littoral platform’ is a 5 to 10 m  
 wide area extending from the inner limit of the  
 littoral vegetation belt (*Juncus* sp., *Tamarix* and  
*Phragmites australis*) to the modern lake shore-  
 line. This area is only occasionally submerged  
 during periods of high lake level. Sediment is  
 mainly composed of light grey, massive, biotur-  
 bated (root casts, worm tracks and mixed sedi-  
 ment textures) coarse silts with abundant plant  
 remains.

The ‘external littoral platform’ (0 to 4.5 m  
 water depth) corresponds to the permanently

COLOUR



28  
 29  
 30  
 31  
 32  
 33  
 34  
 35  
 36  
 37  
 38  
 39  
 40  
 41  
 42 **Fig. 4.** (A) Aerial photograph,  
 43 bathymetry (modified from Ávila  
 44 *et al.*, 1984) and distribution of  
 45 superficial sediment sampling  
 46 points and long cores recovered in  
 47 Lake Estanya, accompanied by den-  
 48 sity maps of: (B) quartz (Qtz) content  
 49 (%), (C) sand content (%) and (D)  
 50 total inorganic carbon (TIC) content  
 51 (%). Interpolation method used for  
 52 mapping was inverse distance to  
 53 weight (IDW) (ARCMAP 9.0®) and 15  
 54 different classes defined at equal  
 55 intervals from minimum to maxi-  
 mum values for each case, were  
 considered (see greyscale legends).



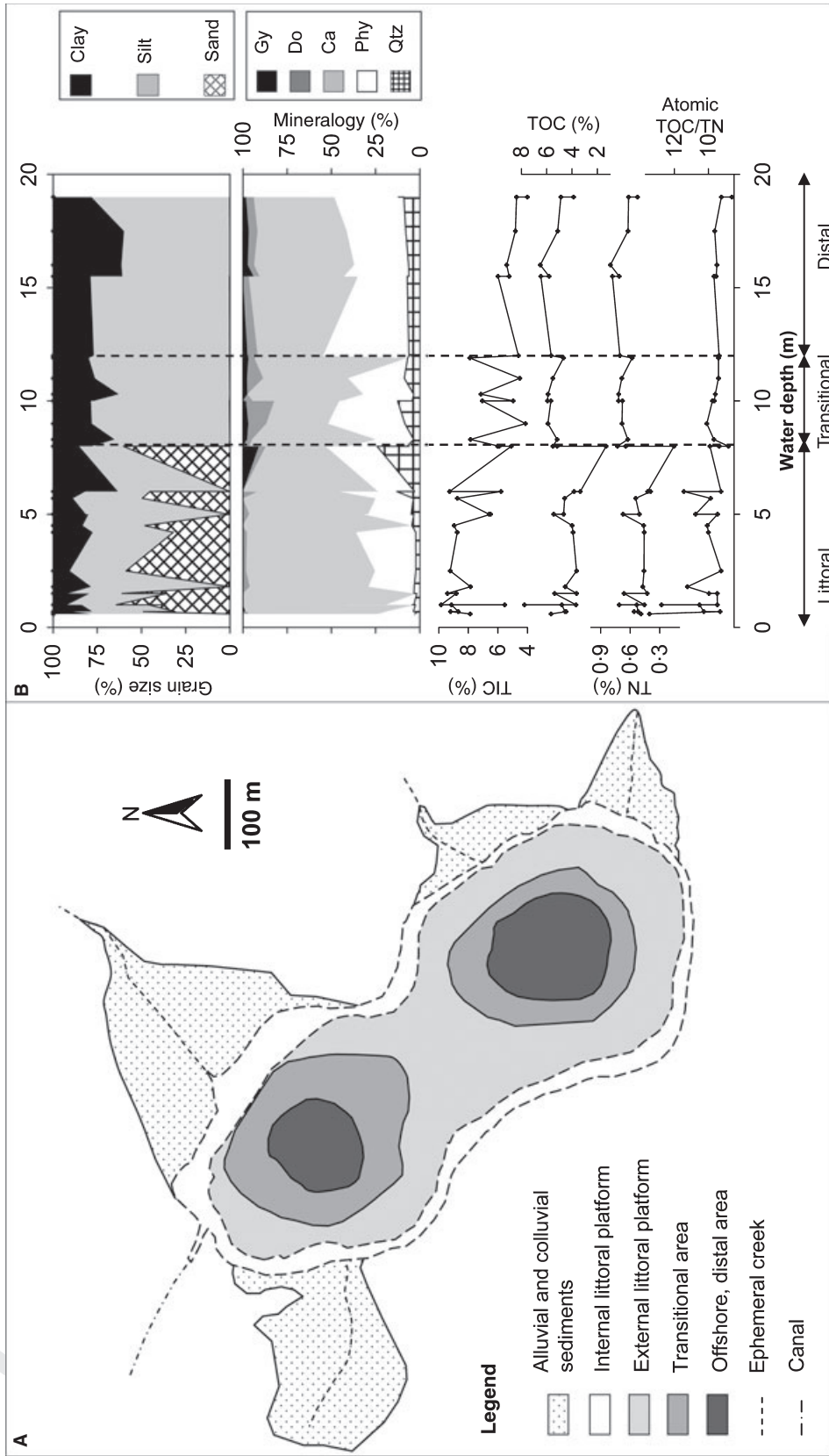


**Fig. 5.** (A) Depositional sub-environments identified in Lake Estanya. (B) Changes in sediment properties (Y-axis) in respect of water depth (m) (X-axis). From top to bottom: grain-size (expressed as percentages of sand, silt and clay fractions), bulk mineralogy (expressed as percentages of quartz (Qtz), phyllosilicates (Phy), calcite (Ca), dolomite (Do) and gypsum (Gy) (see legend); TIC (%), total inorganic carbon, TOC (%), total organic carbon, TN (%), total nitrogen; atomic 12C/14C/TN, total organic carbon/total nitrogen ratio. Depositional sub-environments corresponding to each water-depth interval have also been indicated at the bottom of the panel.



1 submerged, shallow area located between the  
 2 shoreline and the slope. This area has a mean  
 3 width of 50 m around the two sub-basins but  
 4 reaches a width of 200 m on the sill. The prox-  
 5 imal areas of this sub-environment are colonized  
 6 by submerged macrophytes and charophyte  
 7 meadows, which extend offshore. This environ-  
 8 ment is the main carbonate factory in the lake,  
 9 comprising biogenic carbonates (ostracods, gas-  
 10 tropods and *Chara* sp. particles) and non-biogenic  
 11 carbonates (coatings around submerged macro-  
 12 phytes and the lake substrate). Precipitation of  
 13 small calcite crystals in the epilimnion associated  
 14 with algal blooms seems to be a smaller contrib-  
 15 utor to the total carbonate production in the lake.  
 16 Storms and wave activity lead to the reworking of  
 17 these particles, as indicated by the occasional  
 18 presence of ripples in some areas. Sediment is  
 19 composed mainly of banded to massive yellow-  
 20 ish/light grey, bioturbated carbonate-rich (6 to  
 21 10% TIC) silts to fine-grained sands (averaging  
 22 100  $\mu\text{m}$ ) with plant remains (< 4% TOC).

23 (ii) The 'transitional talus' (from 4.5 to 8 m  
 24 water depth) is a narrow area (< 25 m wide)  
 25 characterized by steep morphology, limited pres-  
 26 ence of vegetation as a result of the lack of light  
 27 (Ávila *et al.*, 1984) and the occurrence of small  
 28 mass movements as a result of talus destabiliza-  
 29 tion. Carbonates originating in the littoral plat-  
 30 form are transported to the talus. Sediments are  
 31 dark grey massive silts (averaging 10.5  $\mu\text{m}$ ) with  
 32 carbonates. Mass-wasting processes remobilize  
 33 talus sediments and transport fine detrital mate-  
 34 rial downslope to distal areas.

35 (iii) The 'offshore, distal area' (from 8 to 19 m  
 36 water depth) comprises the central, deepest and  
 37 relatively flat areas characterized by black, mas-  
 38 sive to laminated fine-grained silts (averaging  
 39 10.1  $\mu\text{m}$ ). Sediments are transported as sus-  
 40 pended load to distal areas and by occasional  
 41 mass-wasting processes. The presence of carbon-  
 42 ates is limited (< 5% TIC) because of the large  
 43 distance to the producing littoral areas and to the  
 44 dissolution processes that remove small carbon-  
 45 ate particles. This sub-environment is affected by  
 46 seasonal anoxic hypolimnetic conditions (Ávila  
 47 *et al.*, 1984) and, thus, bioturbation processes are  
 48 greatly reduced or absent. The presence of SRB  
 49 previously reported by numerous studies at this  
 50 site (Esteve *et al.*, 1983; Guerrero *et al.*, 1987; Mir-  
 51 Puyuelo, 1997; Ramírez-Moreno, 2003) favours  
 52 sulphide formation in the summer season and is  
 53 responsible for the characteristic dark colour of  
 54 the sediments and relatively high OM preserva-  
 55 tion (4 to 6% TOC). Although the mixing period

of the water column may last from September to  
 March (Ávila *et al.*, 1984), the footprint of sum-  
 mer anoxic conditions with prevailing oxygen  
 and light-depleted conditions, characterize the  
 deeper sediments. Oxidic/anoxic cycles are only  
 locally recognized at some sampling points where  
 alternating black and dark grey laminations are  
 observed.

Lake basin topography, water depth and dis-  
 tance to shore appear to be the main factors  
 controlling the distribution of present-day surface  
 sediments in the lake. Grain-size obviously is  
 controlled by the distance to shore, showing a  
 decreasing trend towards the distal areas (Figs 4  
 and 5B). Carbonates are more abundant in the  
 littoral and transitional areas and less abundant  
 in the deepest areas, in part due to dissolution  
 processes and distance to shore. OM content in  
 the littoral platform decreases towards the tran-  
 sitional area and it is a mixture of terrestrial,  
 submerged macrophytes and algal material. The  
 organic content increases again in distal areas as a  
 result of the higher preservation potential pro-  
 vided by seasonally anoxic conditions. Distal OM  
 is characterized by comparatively low atomic  
 TOC/TN ratios (9.3 versus 10.4) indicating a  
 higher contribution of algal sources (Meyers,  
 1997; Meyers & Lallier-Vergès, 1999).

#### *Core sedimentary facies*

Ten facies have been defined and correlated  
 within the five long sediment cores recovered at  
 the offshore, distal areas of the two Lake Estanya  
 sub-basins, based on detailed sedimentological  
 descriptions, smear-slide microscopic observa-  
 tions and compositional analyses. According to  
 compositional criteria, these facies have been  
 grouped into four main categories as: (i) clastic;  
 (ii) organic-rich; (iii) carbonate-rich; and (iv)  
 gypsum-rich facies (Table 4A, Fig. 6A).

The clastic facies includes banded to lami-  
 nated, silty and clayey sediments composed of  
 clay minerals, calcite and quartz, with minor  
 amounts of dolomite, feldspars, high magnesium  
 calcite (HMC), pyrite and occasionally gypsum  
 and aragonite. Organic content is relatively low,  
 although with a large range (1 to 7% TOC) and  
 comprises amorphous lacustrine OM, diatoms  
 and occasional macrophyte remains. These sedi-  
 ments are derived from the weathering and  
 erosion of the soils and bedrock in the watershed  
 and are transported to the lake. There are also  
 minor amounts of endogenic material reworked  
 from the littoral carbonate-producing environ-  
 ments.

**Table 4.** Main sedimentological and mineralogical features, compositional parameters (TIC, TOC, TN and TOC/TN ratio, expressed as minimum to maximum intervals) and inferred depositional environments and sub-environments for the different facies and sub-facies defined for: (A) Lake Estanya sedimentary sequence (modified from Morellón *et al.*, 2008); (B) present-day depositional sub-environments and equivalent facies in the core sequence.

| Facies | Sedimentological features   | Compositional parameters  | Depositional subenvironment  |
|--------|---|---|--|
| A      |   |   |  |
| 1      | <b>Blackish, banded carbonate clayey silts</b> Clay-rich matrix mainly composed of phyllosilicates and silty fraction composed of calcite, quartz and dolomite. Minor amounts of feldspars, high-magnesium calcite (HMC) and gypsum. Frequent biogenic components as aggregates of amorphous lacustrine organic matter, macrophyte remains and diatoms. | TIC = 1.95 to 3.60%<br>TOC = 2.25 to 7.40%<br>TN = 0.25 to 0.70%<br>TOC/TN = 6.90 to 11.2 | Deep, monomictic, seasonally stratified freshwater to brackish lake  |
| 2      | <b>Grey, banded to laminated calcareous silts</b> Calcite, quartz and dolomite silt-sized particles embedded in a clay-rich matrix. Minor amounts of feldspars, HMC, pyrite and gypsum. Presence of biogenic components: diatoms, amorphous lacustrine organic matter and land-derived plant remains (frequent).  | TIC = 1.50 to 4.25%<br>TOC = 0.85 to 4.20%<br>TN = 0.10 to 0.45%<br>TOC/TN = 6.15 to 15.5 | Deep, monomictic, seasonally stratified, freshwater to brackish lake |
| 3      | <b>Black, massive to faintly laminated silty clay</b> Clay-rich matrix dominant, with silt-sized calcite and quartz particles and frequent amorphous lacustrine organic matter aggregates. Minor amounts of dolomite, feldspars, HMC and gypsum.  | TIC = 2.15 to 3.10%<br>TOC = 0.95 to 2.10%<br>TN = 0.10 to 0.2%<br>TOC/TN = 7.40 to 10.5  | Flood and/or turbiditic events<br>Deep, dimictic, freshwater lake    |

*Clastic facies*

**Table 4.** (Continued)

| Facies                | Sedimentological features  | Compositional parameters  | Depositional subenvironment                        |
|-----------------------|--|---|--|
| Organic-rich facies   | 4 <b>Brown, massive to faintly laminated sapropel with gypsum</b><br>Organic sediments are composed of amorphous lacustrine organic matter, diatoms and some macrophyte remains, with minor amounts of clay minerals, calcite, dolomite and quartz. Gypsum laminae are composed of idiomorph, well-developed crystals ranging from 25 to 50 µm; mm to 1 cm-sized nodules also occur within the sediment  | TIC = 0 to 11.55%<br>TOC = 0.90 to 24.3%<br>TN = 0.05 to 1.95%<br>TOC/TN = 5.35 to 25.45  | Shallow saline lake                                |
|                       | 5 <b>Variiegated finely laminated microbial mats with aragonite and gypsum</b><br>Sets of dark-brown laminae (lacustrine organic matter, diatoms), yellowish millimetre-thick laminae (authigenic carbonates (calcite, aragonite, dolomite)), and occasional grey carbonate silt laminae.  | TIC = 0 to 8.30%<br>TOC = 5.35 to 21.5%<br>TN = 0.50 to 1.75%<br>TOC/TN = 9.05 to 21.5    | Moderately deep saline lake with light penetration |
| Carbonate-rich facies | 6 <b>Grey and mottled, massive carbonate silt with plant remains and gypsum</b><br>Calcite is dominant, followed by clay minerals, dolomite and quartz and minor amounts of HMC and gypsum. Gypsum nodules and bioturbation features (root traces, coarse plant remains, mottling, mixed sediment textures) are common. Abundant gastropods and large mm to cm-size terrestrial plant remains.   | TIC = 0.85 to 7.25%<br>TOC = 1.00 to 5.85%<br>TN = 0.10 to 0.50%<br>TOC/TN = 6.2 to 22.70 | Ephemeral saline lake–mud flat                     |
|                       | 7 <b>Grey, banded to laminated carbonate-rich silts</b><br>Silt-sized particles of biogenic carbonates ( <i>Chara</i> particles, gastropods) and minor amounts of quartz and plant remains included in a fine-grained matrix composed of authigenic carbonates (rice shaped and rhomboids) and phyllosilicates with gastropods and charophyte particles. Frequent intercalations of centimetre-thick grey coarser, sandy layers mainly composed of reworked biogenic carbonates. | TIC = 1.40 to 9.90%<br>TOC = 0.44 to 2.80%<br>TN = 0.03 to 0.16%<br>TOC/TN = 5.11 to 38.3 | Shallow, carbonate-producing lake                  |

Table 4. (Continued)

| Facies                       | Sedimentological features  | Compositional parameters  | Depositional subenvironment                             |
|------------------------------|--|---|---|
| 8                            | <b>Variagated, finely laminated gypsum, carbonates and clay</b><br>Decimetre-thick intervals composed of millimetre-thick white carbonate-rich laminae, yellowish gypsum-rich laminae and grey massive, clay-rich laminae. Frequent intercalations of brown, mm to centimetre-thick lacustrine organic-rich laminae and massive, centimetre-thick yellowish and light brown, massive coarse-grained silts organized in fining-upwards sequences composed of reworked gypsum and carbonate grains | TIC = 1.70 to 7.10%<br>TOC = 0.45 to 2.40%<br>TN = 0.06 to 0.18%<br>TOC/TN = 6.9 to 23.15   | Deep, saline, permanent lake with saline stratification |
| 9                            | <b>Variagated, banded gypsum, carbonates and clay</b><br>Sets of centimetre-thick alternating yellowish bands of gypsum with reworked biogenic carbonates, dark brown diatom ooze with lacustrine organic matter and lenticular gypsum and grey massive clays.   | TIC = 0.10 to 7.15%<br>TOC = 0 to 4.67%<br>TN = 0.04 to 0.28%<br>TOC/TN = 0 to 12.98  | Deep saline lake  |
| 10                           | <b>Yellowish, massive, coarse-grained gypsum</b><br>Millimetre to centimetre-thick rounded gypsum nodules embedded in a fine-grained silty matrix with lacustrine organic matter, reworked biogenic carbonates, 100 to 200 µm lenticular gypsum crystals and diatoms.  | TIC = 0.38 to 2.60%<br>TOC = 0 to 1.32%<br>TN = 0.03 to 0.1%<br>TOC/TN = 0 to 12.45   | Ephemeral saline lake–mud flat                          |
|                              | Sedimentary sequence equivalent facies   | Compositional parameters  | Depositional subenvironment                             |
| B                            | A 3  | <b>Black, massive to laminated fine-grained silts</b><br>TIC = 4 to 7.90%<br>TOC = 3.90 to 6.50%<br>TN = 0.50 to 0.8%<br>TOC/TN = 7.40 to 8.30  | Offshore, distal area                                   |
| <i>Clastic facies</i>        | B 2  | <b>Dark grey massive silts with carbonates</b><br>TIC = 4.15 to 7.85%<br>TOC = 5.20 to 5.95%<br>TN = 0.60 to 0.73%<br>TOC/TN = 7.55 to 8.65   | Transitional area                                       |
| <i>Carbonate-rich facies</i> | C 7  | <b>Banded to massive yellowish/light grey, carbonate-rich silts with plant remains and abundant bioturbation textures.</b><br>TIC = 5.10 to 9.85%<br>TOC = 1.30 to 7.75%<br>TN = 0.15 to 0.70<br>TOC/TN = 7.9 to 11.5 | Littoral platform                                       |



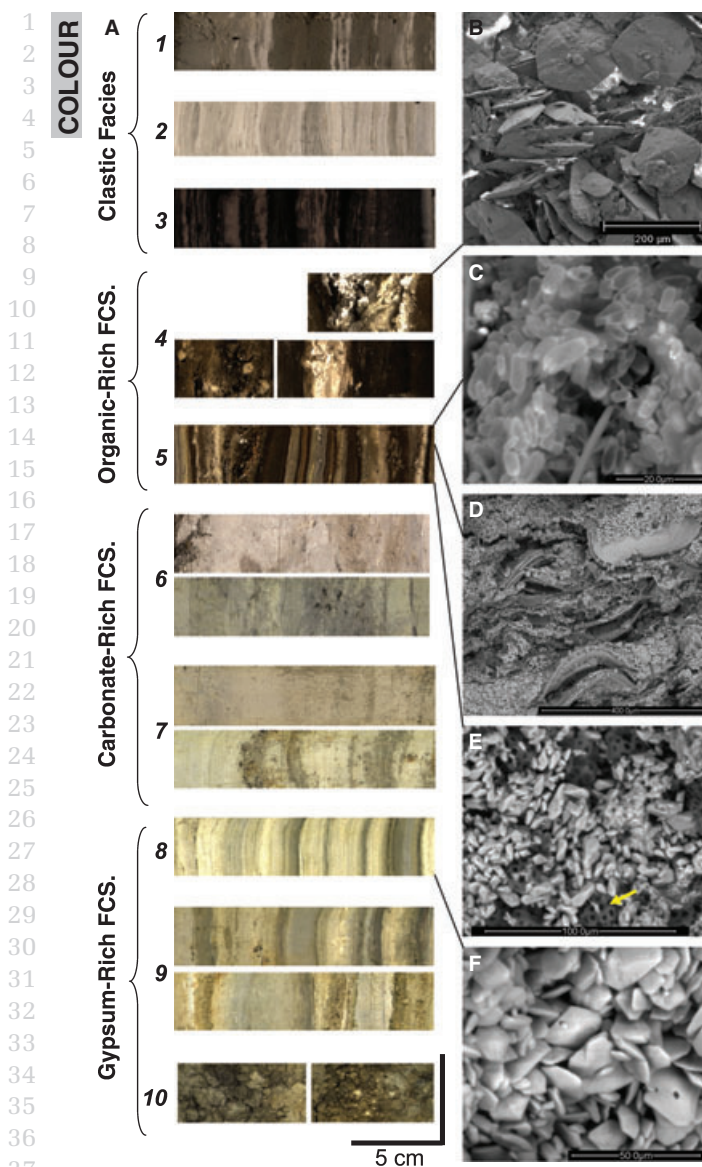


**Fig. 6.** (A) High-resolution core-scan images of sediment sections corresponding to the 10 different facies defined for the Lake Estanya sequence. (B) Secondary electron image; (C to F) Backscattered scanning electron images of sediment textures in selected intervals. (B) Lenticular gypsum crystals generated by intra-sedimentary growth up to 200  $\mu\text{m}$  in size (in facies 4), (C to E) Facies 5. (C) Calcium carbonate crystals forming yellow laminae (in facies 5). (D) Gypsum crystals with *Botryococcus* colonies and diatoms in organic lamina. (E) Enlargement of prismatic gypsum crystals and *Botryococcus* (indicated by an arrow). (F) Lenticular (up to 25  $\mu\text{m}$  long) gypsum crystals from facies 8.

The carbonate-rich facies occurs as banded to laminated decimetre-thick silt layers with massive, sandy intercalations. Sediments are composed mainly of calcite as well as minor amounts of quartz and clay minerals. Carbonates are

biogenic grains (*Chara* fragments, micrite oncoids), carbonate coatings and small crystals derived either from direct precipitation in the epilimnion or from the reworking of particles produced in the littoral environments. Dolomite is less than 10% except in some massive and laminated facies (15 to 20% range).

The organic-rich facies occurs as finely laminated sediments in centimetre-thick to decimetre-thick layers composed of: (i) gypsum-rich sapropels with organic layers and gypsum laminae and nodules (Fig. 6A and B); and (ii) finely laminated, variegated intervals including several laminae types: microbial mats, organic ooze, carbonate (aragonite, calcite, HMC and dolomite), prismatic and nodular gypsum and occasionally clay (Fig. 6A, C, D and E).

The gypsum-rich facies is dominated by endogenic gypsum crystals or nodules. These nodules occur as: (i) finely laminated, variegated gypsum and carbonate mud layers; (ii) banded gypsum and carbonate mud layers; and (iii) irregular centimetre-thick nodular gypsum layers, mostly composed of accumulations of 300  $\mu\text{m}$  lenticular gypsum crystals (Fig. 6A and F).

Riera *et al.* (2004) described a 1.57 m long sediment sequence retrieved in the sill between the two sub-basins in 1.5 m of water depth (Fig. 7). This sequence is composed of laminated carbonate facies alternating with massive reworked carbonate sands and gypsum-rich layers; they both are equivalent to the carbonate-rich and gypsum-rich facies, respectively, described in this facies model (Table 4). Analogously, the three main facies previously described for the present-day depositional sub-environments have their equivalents in the facies model (Table 4B) (see below).

## Core stratigraphy and chronology

### *The sedimentary sequence*

Correlation between all the cores was based on lithology and magnetic susceptibility (Fig. 7). A composite sequence for Lake Estanya has been obtained using cores 1A and 5A (Fig. 8). Although the sediment–water interface was not preserved in core 1A, the upper part of the sequence was reconstructed using a short core correlated using OM and carbonate values (Morellón *et al.*, 2008). The upper 22 cm of the short core 0A were added to core 1A to complete the sequence (Fig. 9).

The Lake Estanya sequence has been divided into seven main sedimentary units and 28 sub-

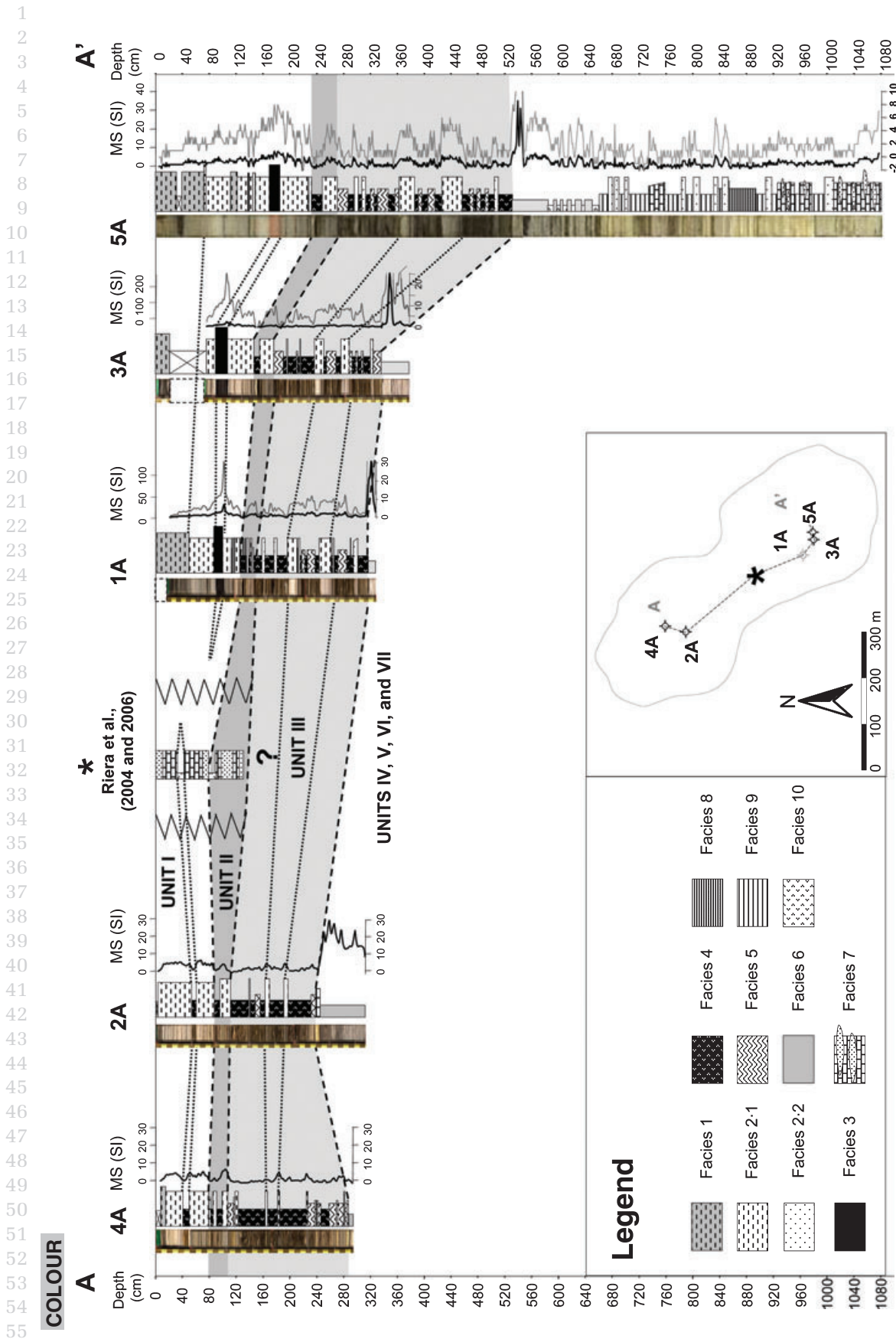


**Fig. 7.** Lithostratigraphic correlation panel of the five cores recovered in Lake Estanya Basin for this research (1A, 2A, 3A, 4A and 5A) and littoral core studied by Riera *et al.* (2004). Core images are accompanied by simplified sedimentological profiles and magnetic susceptibility (MS) core logs. In cores 1A, 3A and 5A, MS core logs are represented in two scales (thick black logs correspond to the upper scale, whereas grey logs correspond to the lower scale, in each case). Dashed horizontal lines represent correlation between main sedimentary units and dotted lines represent correlation between some sedimentary sub-units.



1  
2  
3  
4  
5  
6  
7  
8  
9  
10  
11  
12  
13  
14  
15  
16  
17  
18  
19  
20  
21  
22  
23  
24  
25  
26  
27  
28  
29  
30  
31  
32  
33  
34  
35  
36  
37  
38  
39  
40  
41  
42  
43  
44  
45  
46  
47  
48  
49  
50  
51  
52  
53  
54  
55

**COLOUR**

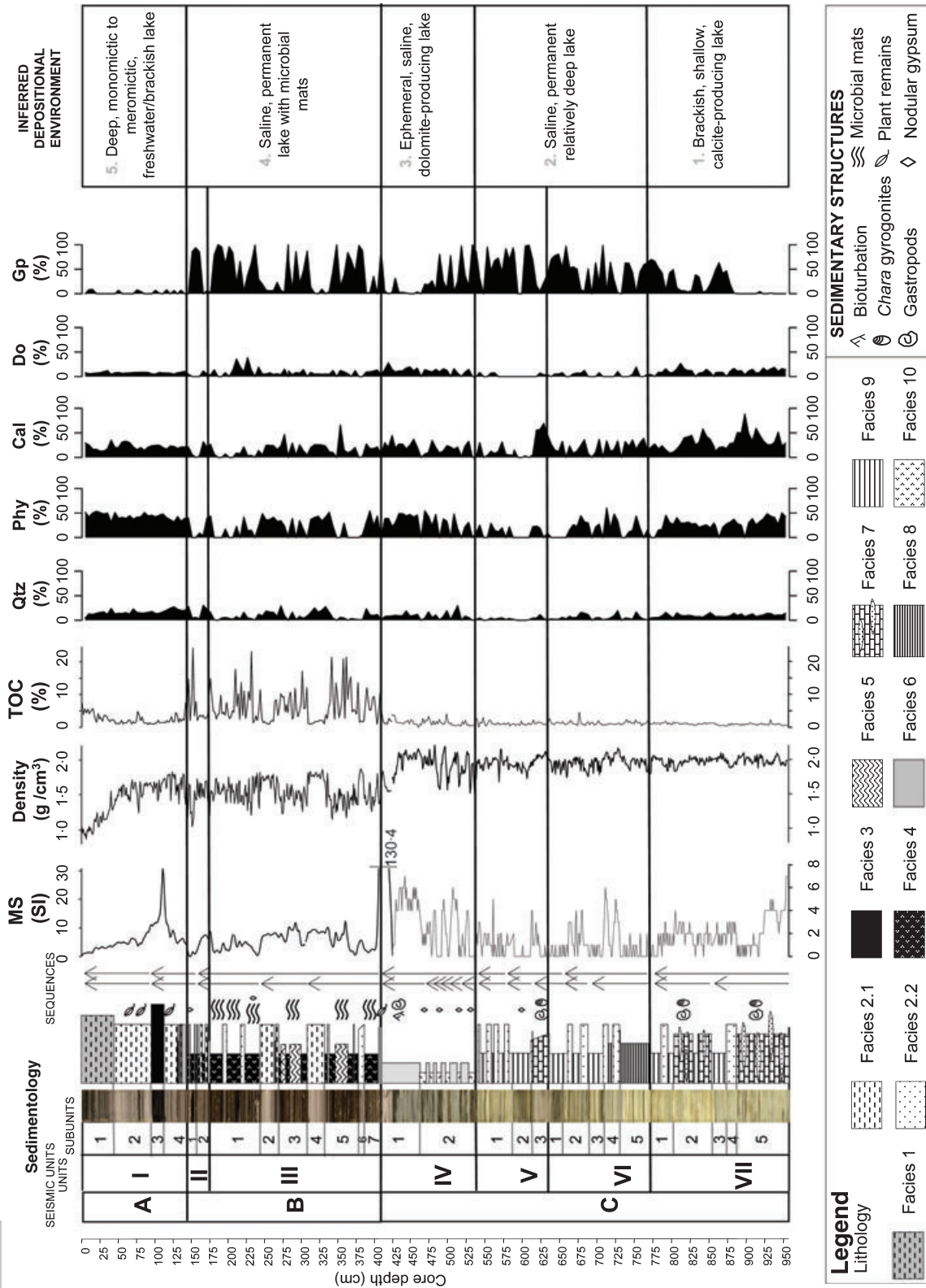


**Fig. 8.** Composite sequence of Lake Estanya sedimentary record formed by cores 1A and 5A. From left to right: seismic units, sedimentary units and sub-units, core images, sedimentological profile with sedimentary structures and interpreted sequences, magnetic susceptibility (MS) (SI units), density (g cm<sup>-3</sup>), total organic carbon (TOC) (%), main mineralogical content (%), including quartz (Qtz), phyllosilicates (Phy), calcite (Cal), dolomite (Do) and gypsum (Gp) and the five inferred stages in the evolution of the lake basin. See legend below for facies and sedimentary structures symbols.

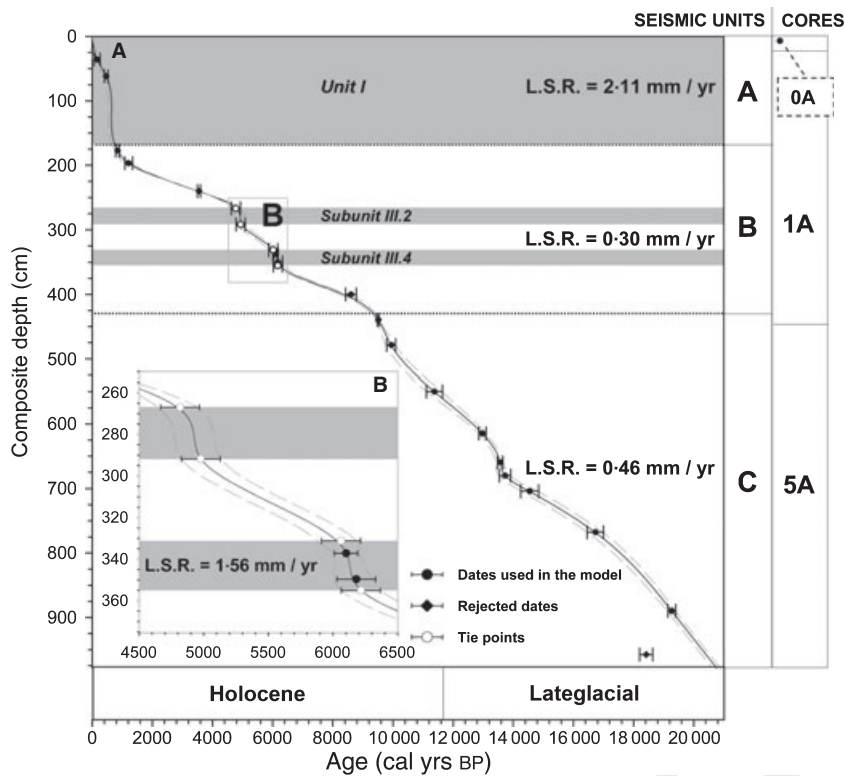


**Fig. 9.** (A) Chronological model of the composite sequence of Lake Estanya, formed by long cores 1A and 5A and short core 0A, based on mixed effect regression function (Heegaard *et al.*, 2005) of 17 accelerator mass spectrometry  $^{14}\text{C}$  dates (black dots) and four tie points (white dots). A reversal date (diamond) is also represented (see legend at the right bottom). Continuous line represents the age–depth function framed by dashed lines (error lines). Horizontal dotted lines indicate seismic unit distribution with their corresponding linear sedimentation rates (LSR). Horizontal grey bands represent intervals characterized by clastic-dominant facies. (B) Detail of the four tie points calculated for clastic dominant intervals (sub-units III.2 and III.4) characterized by higher LSRs, inferred from radiocarbon dates analysed in sub-unit III.4.

units, according to their sedimentary facies (Table 4A, Fig. 8). Correlation with the three main seismic units is shown in Figs 3 and 8.

*Unit VII* (957 to 775 cm core depth) corresponds to the lowermost part of seismic unit ‘C’. It is composed of three main facies: carbonate-rich facies 7, gypsum-rich facies 9 and some clastic facies (facies 2.2).

*Unit VI* (775 to 630 cm) corresponds to the mid-part of seismic unit ‘C’ and is characterized by the deposition of variegated, finely laminated gypsum-rich facies 8 at the bottom and banded gypsum-carbonate facies 9 with centimetre-thick intercalations of clastic facies 2.2 at the top.

*Unit V* (630 to 536 cm) corresponds to the mid to upper part of seismic unit ‘C’. The base of the unit is defined by a thick (25 cm) fining upward, carbonate facies 7 interval. The uppermost part of the sequence is characterized by alternating centimetre-thick layers of clastic facies 2.2 and gypsum-rich facies 9.

*Unit IV* (536 to 409 cm) corresponds to the uppermost part of seismic unit ‘C’ and it has been divided into two distinct intervals. The bottom part is characterized by alternating centimetre-thick bands of massive nodular gypsum facies 10 and carbonate, dolomite-rich facies 6; and the top section, where massive, carbonate–dolomite facies 6 are dominant.

*Unit III* (409 to 176 cm) corresponds to the lower and middle part of seismic unit ‘B’, and it is characterized by organic and gypsum facies 4 and 5 alternating with intercalations of banded clastic facies 2.1. The alternation of facies with the highest magnitude density changes is well-marked by the dense spacing of reflections of seismic unit ‘B’ (Fig. 3A).

*Unit II* (176 to 146 cm) comprises a lower facies 2.1 clastic-dominant sub-unit and an organic-rich interval with a centimetre-thick gypsum-rich sapropel intercalation (facies 4). This abrupt facies change has also been recorded by changes in the physical properties and as high-amplitude reflections in the seismic profiles.

*Unit I* (146 to 0 cm) overlies the mass-wasting deposit in the south-east sub-basin and it corresponds to seismic unit ‘A’, characterized by a lower density of reflections and predominant transparent seismic facies (Fig. 3A). The unit is composed of siliciclastic facies 1, 2.1 and 3. The base of the unit is composed of facies 2.1 with intercalation of millimetre-thick to centimetre-thick plant debris laminae. Intervals characterized by transparent seismic facies correspond to stable density values (lower half of the unit), whereas high amplitude reflections correspond to abrupt changes in the density values (top of the sequence) (Fig. 3A).



### Age model

To construct the age model of the Estanya sequence, 17 radiocarbon dates from cores 1A and 5A (Table 3) were used. The reservoir effect is related to lake dynamics and is unlikely to remain constant through time. Unit I shows a similar depositional environment to recent lake conditions and, consequently, the same  $-585 \pm 60$   $^{14}\text{C}$  years reservoir effect has been applied. A reservoir effect correction of  $-820 \pm 100$   $^{14}\text{C}$  years was applied to bulk sediment samples corresponding to Units II to VI (Table 2). In Unit VIII, bulk OM age is  $940 \pm 170$  years younger than a terrestrial organic macrorest at the same core depth, suggesting reworking from older deposits; both dates were rejected for the construction of the age model.

Linear sedimentation rates (LSR) obtained for clastic-dominant intervals ranging from  $1.5$  (sub-unit III.4) to  $2$   $\text{mm year}^{-1}$  (Unit I) are much higher than those obtained for the rest of the sequence ( $0.2$  to  $0.5$   $\text{mm year}^{-1}$ ) (Fig. 9A). Therefore, the LSR obtained from radiocarbon dates located within sub-unit III.4 was extrapolated for the rest of this sub-unit and also for sub-unit III.2, characterized by the same type of sedimentary facies. Thus, four tie points constraining the base and top of both clastic dominant intervals were obtained and introduced to improve the accuracy of the age model at these intervals (Fig. 9B).

Finally, the depth–age relationship for the sequence (Fig. 9A) was estimated by means of a generalized mixed-effect regression (Heegaard *et al.*, 2005) of 17 calibrated corrected dates (Table 3) and the four obtained tie points mentioned above. The average confidence interval of the error of the age model is *ca* 150 years. The resultant age–depth model for the Lake Estanya record described in this paper indicates that the *ca* 9.8 m of sediments spans from *ca* 21 000 cal yr BP to the present.

## DISCUSSION

### Depositional history and sedimentary environments during the last 21 ka

Based on seismic stratigraphy and facies associations (Table 3), five main stages can be inferred for the evolution of Lake Estanya during the last 21 kyr (Fig. 10).

### Stage 1: a shallow, carbonate-producing lake during the Last Glacial Maximum (21 to 17.3 kyr BP)

The karstification processes and collapse that created the two sinkholes occurred more than 20 kyr ago, prior to the deposition of Unit VII. The seismic survey shows that, during this early stage, deposition was restricted to the central areas of both sub-basins that remained predominantly disconnected until the onset of the Holocene (Fig. 3A). The oldest sediments recovered (Unit VII) indicate a relatively shallow carbonate-producing lake system during the Last Glacial Maximum, characterized by deposition of grey, banded to faintly laminated carbonate silts with centimetre-thick sandy lenses (facies 7).

This facies formed in a relatively shallow setting, characterized by the presence of submerged macrophytes and aquatic plants and intense bioturbation in oxic bottom conditions. *Chara* sp. was the main producers of biogenic carbonate particles further reworked by wave action. External clastic input was limited, which may be due to the combination of the presence of a littoral vegetation belt and reduced run-off (Fig. 10).

Similar environments occur in modern littoral zones (facies A) and in the shallow sill areas (facies S1 and S2, Riera *et al.*, 2004). Littoral environments with high carbonate productivity occur in many karstic lakes in the Iberian Peninsula: La Cruz (Romero *et al.*, 2006; Romero-Viana *et al.*, 2008), carbonate-rich wetlands associated with fluvial settings, e.g. Tablas de Daimiel (Álvarez Cobelas & Cirujano, 1996; Domínguez-Castro *et al.*, 2006) or tufa-dammed lakes, as Ruidera (Ordóñez *et al.*, 2005) and Taravilla (Valero Garcés *et al.*, 2008). More examples of these depositional environments can be found elsewhere in the Mediterranean basin, as Lake Vrana (Schmidt *et al.*, 2000) and in many ‘marl’ lakes (Murphy & Wilkinson, 1980; Platt & Wright, 1991).

Fluctuations in lake level and water chemical concentration led to deposition of carbonate (facies 7) and gypsum (facies 9) sequences. Although there is no clear evidence of increased subsidence as a result of karstic processes at this time, the presence of freshwater carbonates could be interpreted as evidence of an early stage of karstic lake development, when the hydrological system was relatively open because the bottom of the lake was not completely sealed off. A short residence time for lake water as a result of a

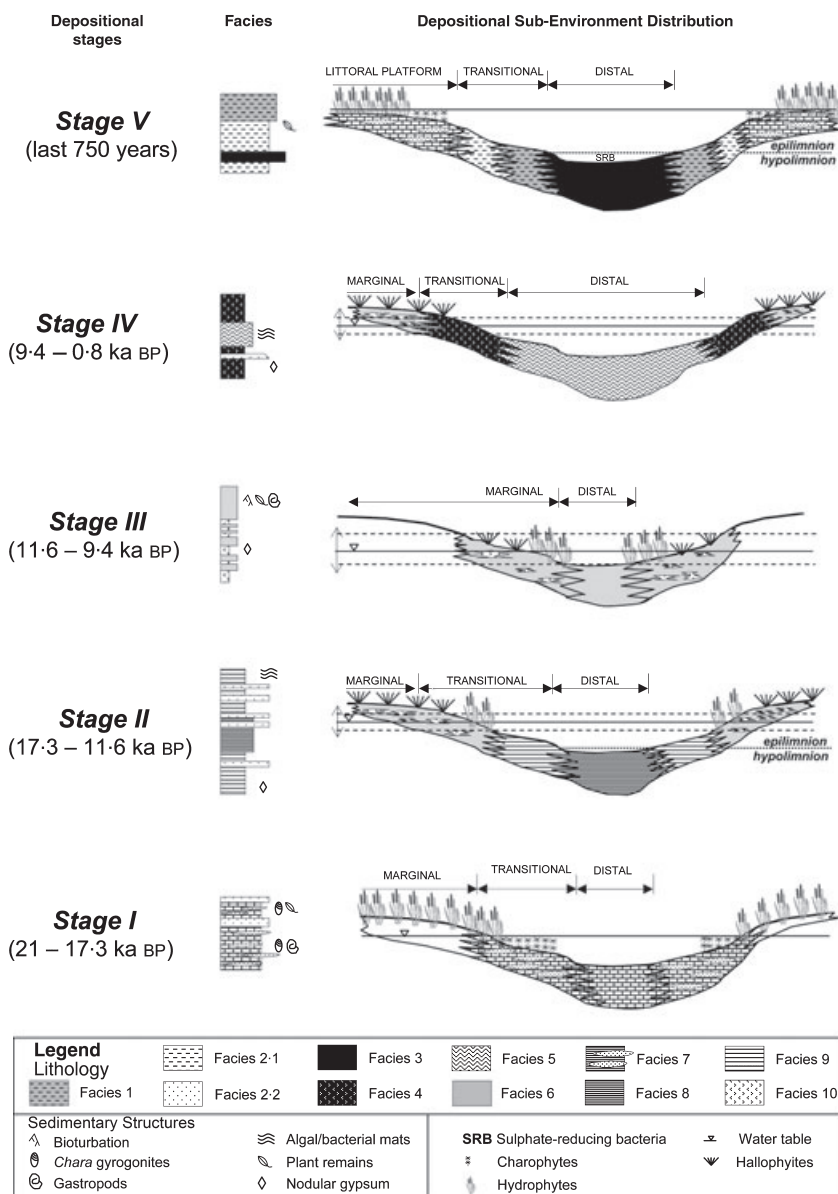


**Fig. 10.** Facies model sketches showing the main depositional environments interpreted for the five main stages identified in the evolution of the Lake Estanya sedimentary record. From bottom to top: Stage I (shallow, carbonate-producing lake); Stage II (permanent, relatively deep, saline lake); Stage III (shallow saline lake–saline mud flat); Stage IV (saline lake with microbial mats); and Stage V (brackish to freshwater, deep lake). For each depositional environment, deposition time-period, facies sequences and depositional sub-environments spatial distribution are also indicated (see legend below).

connection with the aquifer during periods of increased subsidence could explain the absence of evaporite facies at the base of the sequence. Alternatively, the presence of freshwater carbonates could imply a more positive water balance.

*Stage 2: a permanent, relatively deep saline lake during the late glacial (17.3 to 11.6 kyr BP)*  
The occurrence of finely laminated gypsum-rich facies 8 along Units V, VI and VII marks the development of a stratified, saline and relatively deep lake lasting for some millennia. Facies 8 represents primary gypsum deposition (cumulate crystals) in distal areas of a relatively deep saline lake, in which banded carbonate and gypsum silt (facies 9) and clastic facies 2.2 are deposited in

the more littoral areas (Fig. 10). Laminae preservation suggests anoxic environments. Anoxic conditions at the bottom of the lake could have resulted from water stratification induced by a higher salinity in the hypolimnion as found in some lakes in the northern Great Plains (Valero-Garcés & Kelts, 1995; Last & Vance, 1997), where gypsum laminae are also formed.

The development of such a system suggests that the lake basin had been plugged by sediments and leaks to the aquifers became minimal (mature stage) leading to evaporite formation. A progressive regression trend occurred and distal finely laminated facies 8 were gradually replaced by cycles of clastic facies 2.2 (flooding) and gypsum facies 9 (desiccation). At about 13.5 kyr BP,

1 deposition of carbonate-rich facies 7 indicates a  
 2 brief return towards freshwater to brackish con-  
 3 ditions. A shallow saline lake developed after-  
 4 wards characterized by alternating gypsum-rich  
 5 facies 9 and centimetre-thick intercalations of  
 6 massive clastic inputs, represented by facies 2.2.

7  
 8 *Stage 3: a shallow saline lake–saline mudflat*  
 9 *during the transition to the Holocene (from*  
 10 *11.6 ka to 9.4 kyr BP).*

11 During this period, represented by the deposition  
 12 of Unit IV, Lake Estanya was a shallow, ephemer-  
 13 al, saline lake–mud flat with carbonate-domi-  
 14 nated sedimentation during flooding episodes  
 15 (facies 6) and gypsum precipitation as nodules  
 16 and large intrasediment crystals (facies 10) during  
 17 desiccation phases. The occurrence of interstitial  
 18 and intra-sedimentary gypsum crystals and the  
 19 presence of dolomite are characteristic of domi-  
 20 nant shallow conditions with frequent periods of  
 21 subaerial exposure and evaporite pumping pro-  
 22 cesses (Last, 1990). The increase in magnetic  
 23 susceptibility values and the sharp peak at the top  
 24 of the unit reflect both an increase in clastic input  
 25 and the occurrence of oxidation processes coher-  
 26 ent with frequent subaerial conditions (Morellón  
 27 *et al.*, 2008).

28 Examples of this depositional environment can  
 29 be found in marginal playa lake settings charac-  
 30 terized by the deposition of alternating carbonate  
 31 and gypsum-rich interstitial facies (Schreiber &  
 32 Tabakh, 2000). Modern analogues occur at nearby  
 33 sites in the Central Ebro Basin saline lakes, e.g. La  
 34 Playa (Valero-Garcés *et al.*, 2004); Gallocanta  
 35 (Pérez *et al.*, 2002; Rodó *et al.*, 2002; Corzo *et al.*,  
 36 2005); Lake Chiprana (Valero-Garcés *et al.*, 2000)  
 37 as well as in other areas of the Iberian Peninsula  
 38 (Reed, 1998) and the Mediterranean basin (Schre-  
 39 iber & Tabakh, 2000).

41 *Stage 4: a saline lake with abundant microbial*  
 42 *mats during the Holocene (9.4 to 0.8 kyr BP)*

43 The deposition of seismic unit ‘B’ marks a general  
 44 increase in lake level, leading to the connection of  
 45 the two sub-basins. Sedimentary Unit III started  
 46 with deposition of a coarse clastic layer with large  
 47 plant debris, deposited throughout the lake basin  
 48 reflecting a flood episode, responsible for the  
 49 increase of lake level and the establishment of a  
 50 relatively deep saline lake.

51 Two facies are dominant during this stage:  
 52 (i) massive organic ooze with nodular and lentic-  
 53 ular gypsum interpreted as deposition in the  
 54 marginal zones, affected by strong fluctuations in  
 55 lake level and seasonal desiccation (facies 4); and

(ii) variegated, laminated facies 5 interpreted as  
 deposition in the intermediate and distal zones,  
 with more stable lake levels, relatively deep, but  
 with enough light reaching the lake bottom to  
 allow the development of microbial mats. Fre-  
 quent anoxic conditions and saline stratification  
 were conducive to aragonite and gypsum forma-  
 tion and laminae preservation (Valero-Garcés &  
 Kelts, 1995).

Shallow saline lake systems, such as that  
 interpreted for stage 4, are affected strongly by  
 fluctuations in lake level, and littoral areas are  
 affected by frequent seasonal desiccation periods  
 (Last, 1990; Schreiber & Tabakh, 2000). The  
 occurrence of microbial mats is common in these  
 shallow saline systems (Bauld, 1981). The sub-  
 stantial development of benthonic microbial mats  
 with aragonite laminae as distal facies 5 indicates  
 a higher organic productivity than during late  
 glacial times and limits the maximum deposi-  
 tional water depth to a few metres where light can  
 still reach the lake bottom. Thin clastic interca-  
 lations (facies 2.2) such as in sub-unit III.6 mark  
 flood events reaching the centre of the lake,  
 whereas thicker intervals of carbonate–siliciclas-  
 tic facies 2.1, represented by sub-units III.2 and  
 III.4 are interpreted as being deposited during  
 longer periods of increased runoff, occurring  
 during the early and mid-Holocene.

Saline conditions were dominant again after  
 4.8 kyr BP, as indicated by the deposition of  
 gypsum-rich facies 10 and massive sapropels  
 facies 4 (sub-unit III.1); terrigenous input from  
 the catchment was restricted to centimetre-thick  
 clastic intercalations. The abundance of gypsum  
 nodules and the decrease in carbonate content  
 indicate that more saline conditions and shal-  
 lower lake levels lasted until 1.2 kyr BP. Although  
 major changes in sedimentation appear to be  
 synchronous throughout the basin and main units  
 can be easily correlated (Fig. 7), significant lateral  
 facies changes between the two sub-basins occur  
 through Unit III. More proximal facies occur in  
 the north-west sub-basin, where clastic facies are  
 reduced and massive gypsum-rich sapropels  
 (facies 4) are dominant over microbial mats  
 (facies 5) during this period (Fig. 7).

A transition towards less saline conditions,  
 higher lake level and increased runoff is repre-  
 sented by the deposition of Unit II (1200 to  
 870 cal yr BP). This transgressive period was  
 interrupted by the deposition of a thick gypsum  
 layer (Unit II.1), indicating a sharp drop in lake  
 level and more saline conditions around 750 cal  
 yr BP, according to the age model used here.



1 Similar depositional environments can be found  
2 in transitional to distal areas of playa lake  
3 settings, as indicated in examples listed for  
4 previous stage 4.

5  
6 *Stage 5: a brackish to freshwater, deep lake*  
7 *since the 12th century (750 cal yr BP to present)*  
8 The abrupt lake level drop at 750 cal yr BP marked  
9 by the deposition of Unit II coincided with the  
10 emplacement of the mass-wasting unit 'D'. This  
11 deposit is overlain by a thick clastic sequence  
12 (Unit I) continuously deposited throughout the  
13 whole lake basin as indicated by seismic data.  
14 The absence of gypsum deposition and the dom-  
15 inance of fine-grained clastic sedimentation (clastic  
16 facies 1, 2 and 3) indicate lower salinity,  
17 generally higher lake level and an increase in  
18 sediment delivery to the lake. Higher clastic input  
19 is probably related to the development of agriculture  
20 in the area during medieval times (Riera  
21 *et al.*, 2004).

22 Facies and depositional sub-environments are  
23 similar to the present-day distribution. The lake  
24 has considerable water depth and frequent sea-  
25 sonal or permanent anoxic lake bottom condi-  
26 tions. Clastic input from the watershed is high,  
27 and carbonate production is restricted to the  
28 epilimnion and to the littoral areas where it is  
29 the dominant depositional process. Three main  
30 facies associations and sub-environments can be  
31 identified: (i) littoral platform; (ii) transitional  
32 area; and (iii) distal area (Figs 5 and 10). Littoral  
33 and transitional facies would correspond to those  
34 described by Riera *et al.* (2004) in the core from  
35 the sill between the two sub-basins (facies S1 and  
36 S2), and facies A and B identified in the modern  
37 lake survey, all of them corresponding to core  
38 facies 7.

39 Modern analogue systems to this depositional  
40 environment in the Iberian Peninsula are Lake  
41 Banyoles (Julià, 1980); Lake Montcortés (Camps  
42 *et al.*, 1976; Miracle & Gonzalvo, 1979; Modamio  
43 *et al.*, 1988); and Lake Zoñar (Valero-Garcés *et al.*,  
44 2006). Many deep lakes in the karstic regions of  
45 the Mediterranean correspond to this deposi-  
46 tional setting [e.g. Lake Salda, Turkey (Kazanci  
47 *et al.*, 2004); Lake Vrana, Croatia (Schmidt *et al.*,  
48 2000)].

49 Although lake level remained relatively high  
50 during this stage, significant hydrological fluctu-  
51 ations occurred. Deposition of facies 1, charac-  
52 terized by a black colour and high magnetic  
53 susceptibility values as a consequence of  
54 sulphide formation under permanent anoxic  
55 hypolimnetic conditions (Morellón *et al.*, 2008)

probably represents the deepest lake level  
conditions recorded throughout the sequence.  
Deposition of this unit is restricted to the deepest  
south-east basin, indicating that this long-term  
water stratification only affected the deepest areas  
of the lake (Fig. 7). Finally, the deposition of sub-  
units 1 and 2 indicate a shallower sub-envi-  
ronment characterized by a return towards the  
monomictic, seasonal water stratification prevail-  
ing today in Lake Estanya.

### Factors controlling sedimentation in Lake Estanya

The interpretation of the sedimentary sequence  
and the basin architecture of Lake Estanya  
allowed the definition of a depositional model  
characterized by a large variability of facies and  
depositional sub-environments during the last  
21 kyr. Most factors affecting sedimentation in  
lakes responded to internal thresholds, leading to  
abrupt lateral and vertical changes in facies  
(Valero-Garcés & Kelts, 1995). Although most of  
these changes respond to feedback mechanisms  
and they are all inter-related, they are governed  
directly or indirectly by fluctuations in lake level  
and, consequently, the evolution of the basin is  
greatly controlled by the hydrology. However, the  
occurrence of extreme events (floods, mass-was-  
ting processes) and changes in the watershed (land  
use) can also affect the lake dynamics and  
sedimentation patterns. The main factors control-  
ling sedimentation in Lake Estanya are: (i) karstic  
processes; (ii) hydrology; (iii) water salinity; (iv)  
water stratification; (v) clastic input; and (vi)  
mass-wasting processes.

(i) *Karstic processes* (collapse, subsidence and  
dissolution) were responsible for the formation of  
the basin and the functioning of the hydrogeo-  
logical system. Initial lake formation is related  
directly to the karst topography of the bedrock  
and mechanical and dissolution processes that  
generate the accommodation space for the lake  
(Kindinger *et al.*, 1999; Gutiérrez *et al.*, 2008).  
Lateral continuity of the seismic reflections in the  
northern sub-basin indicates that there was no  
significant subsidence during the last 20 kyr.  
Seismic stratigraphy in the southern sub-basin is  
more complex and characterized by strong sedi-  
ment thickness variations and by an irregularly  
shaped acoustic basement probably suggesting  
some collapse activity during the early late glacial  
stage, when the lower part of unit 'C' was  
deposited (transitional phase). Modern Lake  
Estanya fits the category of a mature, base-level

1 phase karst lake, according to the Kindinger *et al.*  
2 (1999) classification.

3 (ii) *The hydrological balance and lake-level*  
4 *fluctuations* are the main factors controlling  
5 facies distribution and composition. In Lake  
6 Estanya, there is no evidence of significant  
7 changes in the hydrogeological behaviour of the  
8 lake system because the basin became sealed-off  
9 during the late glacial. It is assumed that  
10 increased rainfall would have caused increased  
11 groundwater and spring flow in the past.

12 (iii) *Water salinity and chemical composition*  
13 generally varies inversely with water level, as a  
14 result of the hydrological balance (Street-Perrott  
15 & Harrison, 1985). In Lake Estanya, salinity  
16 changes have controlled the precipitation of  
17 different carbonate and sulphate phases and  
18 the development of different biota adapted to  
19 particular conditions. The recycling of previ-  
20 ously deposited salts during saline stages, how-  
21 ever, had a strong impact on the chemical  
22 composition of lake waters and may have led  
23 to decoupling of lake water volume and chem-  
24 ical concentration.

25 (iv) *Water stratification* can be achieved in  
26 karstic lakes through thermal processes and by  
27 large chemical gradients. The development of  
28 seasonal or permanent thermal stratification  
29 requires a minimum water depth of 6 m (Shaw  
30 *et al.*, 2002). Thermal stratification is dominant  
31 in present-day Lake Estanya and seems to have also  
32 been prevalent during the last 800 years. Lake  
33 depth is the main parameter currently controlling  
34 thermal stratification. At this time, permanent  
35 anoxic conditions only developed in the deeper  
36 southern basin leading to deposition of facies 3.  
37 In the northern, shallower sub-basin, only sea-  
38 sonal stratification occurred.

39 However, in the past, chemical processes have  
40 played a major role in water stratification during  
41 both high-lake and low-lake periods. In saline  
42 lakes, meromictic conditions can occur when a  
43 large gradient between denser, chemically con-  
44 centrated waters in the hypolimnion and fresher  
45 waters in the epilimnion is established. There are  
46 numerous examples of relatively deep, meromic-  
47 tic lakes with laminated salt deposition in the  
48 hypolimnion, as stated above. A setting of this  
49 type is interpreted for deposition of the laminated  
50 gypsum-rich facies 8 in Unit VI. Because of a high  
51 chemical concentration, some shallow saline  
52 lakes could also become stratified and anoxic at  
53 the bottom; this would be the case for Lake  
54 Estanya during some depositional intervals of  
55 Unit III.

(v) *Clastic input* mainly depends on external  
parameters, such as the availability of sediments  
in the catchment area, climatic conditions, topo-  
graphy, vegetation cover, land uses, presence of  
littoral vegetation and aquatic macrophytes acting  
as a barrier to sediment delivery. Extreme flood  
events occurred during the last 20 kyr and their  
sedimentological signature (facies 2.2) is found in  
the distal facies of all depositional environments,  
fresh, saline, deep and shallow. However, higher  
general clastic input into the lake only occurs in  
the upper part of Unit I and in sub-units III.2 and  
II.4. The mid Holocene episodes probably are  
associated with periods of higher precipitation  
and runoff. However, the abrupt change in lake  
dynamics during the last 800 years probably is  
a reflection of anthropogenic impact in the  
watershed.

(vi) *Mass-wasting processes* are a common  
feature in lake basins with steep margins  
(Chapron *et al.*, 2004; Girardclos *et al.*, 2007;  
Strasser *et al.*, 2007). Initial local, subaqueous  
slope instabilities are generated when the shear  
stress in the sediments can no longer sustain the  
gravitational downslope forces (Coleman & Prior,  
1988; Hampton *et al.*, 1996). The largest mass-  
wasting deposit identified in the Lake Estanya  
basin is restricted to the south-east sub-basin and  
emplaced prior to the deposition of Unit I. Both  
the external structure, characterized by a wedge  
shape with a lobe-shaped distal termination and  
an irregular lower and upper surface (hum-  
mocky), and the internal structure (transparent  
to chaotic seismic facies), indicates the loss of  
internal structure typical of a mass flow (Schnell-  
mann *et al.*, 2005). This mass-flow deposit  
occurred during a transgressive phase leading to  
higher lake levels and during a period of  
increased sediment delivery to the lake. There  
are many factors responsible for slope instabili-  
ties in lakes: earthquakes (Schilts & Clague, 1992),  
sediment overloading, rapid water level changes,  
cyclic loading by waves and biogenic gas pro-  
duction from the decay of OM (Nisbet & Piper,  
1998). Although the abrupt transition from low-  
lake level and gypsum deposition (Unit II) to  
higher-lake level and clastic deposition (Unit I)  
might have played a role in the generation of this  
deposit, none of the other factors can be ruled out.  
Earthquakes in this sector of the Pyrenean Range  
have been reported during the Holocene (Alasset  
& Meghraoui, 2005; Gutierrez-Santolalla *et al.*,  
2005). In particular, the east-west trending North  
Maladeta Fault, has been identified as the most  
probable source of the Ribagorza earthquake of AD

1 1373 (Olivera *et al.*, 1994, 2006), with an esti-  
 2 mated magnitude of  $M_w$  6.2. Additionally, a  
 3 major change in land-use occurred during medi-  
 4 eeval times (Riera *et al.*, 2004, 2006). It is hypo-  
 5 thesized that a higher sediment load to the lake  
 6 because of increased farming practices during  
 7 higher-lake levels created the conditions condu-  
 8 cive to mass-wasting episodes. Seismic activity  
 9 (the Ribagorza earthquake) could have triggered  
 10 these events.

## 11 CONCLUSIONS

12  
 13 The spatial distribution of sedimentary facies  
 14 in Lake Estanya allows the identification of  
 15 three main depositional sub-environments: (i) the  
 16 littoral carbonate-producing platform; (ii) the tran-  
 17 sitional, steep talus; and (iii) the offshore, distal  
 18 area. The distribution of these sub-environments is  
 19 conditioned strongly by lake bathymetry, which  
 20 today exerts a key influence on the depositional  
 21 conditions.

22  
 23 As in most small relatively deep karstic lakes,  
 24 the main factors controlling sedimentation are:  
 25 hydrological balance and lake-level changes,  
 26 water salinity and chemical composition, water  
 27 stratification, clastic input and the occasional  
 28 occurrence of mass-wasting and karstic activity.  
 29 The interplay of these processes during the  
 30 depositional history results in a complex vertical  
 31 and lateral alternation of 10 different sedimentary  
 32 facies, indicative of five different depositional  
 33 environments. A brackish, shallow, calcite-pro-  
 34 ducing lake was established during the full  
 35 glacial period, probably after a period of in-  
 36 creased karstic (solution and collapse) activity  
 37 that created more accommodation space in the  
 38 basin. When the lake basin was completely  
 39 sealed-off, a permanent, saline, relatively deep  
 40 lake developed during the late glacial. A shallow,  
 41 brackish to saline, ephemeral, dolomite-produc-  
 42 ing lake occurred during the transition to the  
 43 Holocene and was substituted by a saline shallow  
 44 lake with microbial mats, lasting from the early to  
 45 the late Holocene. Finally, changes in land use of  
 46 the watershed and a rise in lake level induced a  
 47 large increase in sediment input to the lake. Thus,  
 48 a freshwater to brackish, permanent, deep mero-  
 49 mictic to monomictic lake similar to the present-  
 50 day conditions remained during the last  
 51 800 years.

52  
 53 The sedimentary facies model defined for Lake  
 54 Estanya, integrated with seismic stratigraphy,  
 55 provided a detailed reconstruction of the deposi-

tional history of the basin showing abrupt and  
 large hydrological changes during the last 21 kyr.  
 Further research will clarify the timing and extent  
 and of the environmental changes archived in  
 this lake sequence.

## ACKNOWLEDGEMENTS

Financial support for research was provided by  
 the Spanish Inter-Ministry Commission of Sci-  
 ence and Technology (CICYT), through the pro-  
 jects LIMNOCLIBER (REN2003-09130-C02-02),  
 IBERLIMNO (CGL2005-20236-E/CLI), LIMNO  
 CAL (CGL2006-13327-C04-01) and GRACCIE  
 (CSD2007-00067). Additional funding was pro-  
 vided by the Instituto de Estudios Altoaragoneses  
 (IEA). The Aragonese Regional Government-CAJA  
 INMACULADA partially funded XRD analyses,  
 seismic studies and XRF analyses at University of  
 Cádiz, ETH-Zurich, University of Geneva and MA-  
 RUM Centre (University of Bremen), respectively,  
 by means of two travel grants.

M. Morellón is supported by a PhD contract  
 with the CONAI+D (Aragonese Scientific Council  
 for Research and Development), A. Moreno holds  
 a ESF – Marie Curie programme post-doctoral  
 contract, Maite Rico holds a ‘Juan de la Cierva’  
 contract from the Spanish Government and Juan  
 Pablo Corella holds a CONAI+D PhD fellowship.  
 We are indebted to Anders Noren, Doug Schnur-  
 renberger and Mark Shapley (LRC-University of  
 Minnesota) for the 2004 coring campaign and  
 Santiago Giral and Armand Hernández  
 (IJA-CSIC), as well as Alberto Sáez and J.J.  
 Pueyo-Mur (University of Barcelona) for coring  
 assistance in 2006. We are also grateful to ETH-  
 Zürich, University of Geneva, MARUM centre  
 (University of Bremen), IGME, EEAD-CSIC and  
 IPE-CSIC laboratory staff for their collaboration in  
 this research. We thank anonymous reviewers  
 and Associate Editor, Stephen Lokier, for their  
 helpful comments and their criticism, which led  
 to a considerable improvement of the manuscript.

## REFERENCES

- Alagöz, C.A. (1967) *Jips karst Olaylari – Les phénomènes karstiques du gypse aux environs et à l'est de Sivas*. Ankara Universitesi Pasimevi, ????, 126 pp.
- Alasset, P.-J. and Meghraoui, M. (2005) Active faulting in the western Pyrenees (France): paleoseismic evidence for late Holocene ruptures. *Tectonophysics*, **409**, 39–54.
- Álvarez Cobelas, M. and Cirujano, S. (1996) *Las Tablas de Daimiel*. Ecología acuática y sociedad, Madrid, 23–29 pp.



- 1 Anselmetti, F.S., Ariztegui, D., Hodell, D.A., Hillesheim, M.B.,  
 2 Brenner, M., Gilli, A., McKenzie, J.A. and Mueller, A.D.  
 3 (2006) Late Quaternary climate-induced lake level variations  
 4 in Lake Peten Itza, Guatemala, inferred from seismic  
 5 stratigraphic analysis. *Palaeogeogr. Palaeoclimatol. Palaeo-*  
 6 *ecol.*, **230**, 52–69.
- 7 Ávila, A., Burrell, J.L., Domingo, A., Fernández, E., Godall, J.  
 8 and Llopart, J.M. (1984) Limnología del Lago Grande de  
 9 Estanya (Huesca). *Oecologia Aquatica*, **7**, 3–24.
- 10 Balch, D.P., Cohen, A.S., Schnurrenberger, D.W., Haskell, B.J.,  
 11 Valero Garcés, B.L., Beck, J.W., Cheng, H. and Edwards, R.L.  
 12 (2005) Ecosystem and paleohydrological response to Quaternary  
 13 climate change in the Bonneville Basin, Utah. *Palaeogeogr. Palaeoclimatol. Palaeoecol.*, **221**, 99–122.
- 14 Bauld, J. (1981) Occurrence of benthic microbial mats in saline  
 15 lakes. *Hydrobiologia*, **81–82**, 87–111.
- 16 Bohacks, K.M., Carroll, A.R., Neal, J.E. and Mankiewicz, P.J.  
 17 (2000) Lake-basin type, source potential, and hydrocarbon  
 18 character: an integrated-sequence-stratigraphic-geochemical  
 19 framework. In: *Lake Basins Through Space and Time* (Eds  
 20 E.H. Gierlowski-Kordesch and K.R. Kelts), *AAPG Stud. Geol.*, **46**, 3–34.
- 21 Bourrouilh-Le Jan, F.G., Beck, C. and Gorsline, D.S. (2007)  
 22 Catastrophic events (hurricanes, tsunamis and others) and  
 23 their sedimentary records: introductory notes and new  
 24 concepts for shallow water deposits. *Sed. Geol.*, **199**, 1–11.
- 25 Bradley, R.S., Hughes, M.K. and Diaz, H.F. (2003) Climate  
 26 change: climate in medieval time. *Science*, **302**, 404–405.
- 27 Brown, E.T., Johnson, T.C., Scholz, C.A., Cohen, A.S. and  
 28 King, J.W. (2007) Abrupt change in tropical African climate  
 29 linked to the bipolar seesaw over the past 55 000 years.  
 30 *Geophys. Res. Lett.* **34**, doi: 10.1029/2007GL031240.
- 31 Buurman, P., Pape, T. and Muggler, C.C. (1997) Laser grain-  
 32 size determination in soil genetic studies: I. *Pract. probl. Soil Sci.*, **162**, ???.
- 33 Camps, J., Gonzalvo, I., Güell, J., López, P., Tejero, A., Toldrà,  
 34 X., Vallespinos, F. and Vicens, M. (1976) El lago de Mont-  
 35 cortès, descripción de un ciclo anual. *Oecologia Aquatica*, **2**, 99–110.
- 36 Chapron, E., Van Rensbergen, P., De Batist, M., Beck, C. and  
 37 Henriot, J.P. (2004) Fluid-escape features as a precursor of a  
 38 large sub-lacustrine sediment slide in Lake Le Bourget, NW  
 39 Alps, France. *Terra Nova*, **16**, 305–311.
- 40 Chung, F.H. (1974a) Quantitative interpretation of X-ray dif-  
 41 fraction patterns of mixtures. I. Matrix-flushing method for  
 42 quantitative multicomponent analysis. *J. Appl. Crystallogr.*, **7**, 000.
- 43 Chung, F.H. (1974b) Quantitative interpretation of X-ray dif-  
 44 fraction patterns of mixtures. II. Adiabatic principle of X-ray  
 45 diffraction analysis of mixtures. *J. Appl. Crystallogr.*, **7**, 526–  
 46 531.
- 47 Cohen, A.S. (2003) *Paleolimnology: The History and Evolution*  
 48 *of Lake Systems*. Oxford University Press, New York, 500 pp.
- 49 Coleman, J.M. and Prior, D.B. (1988) Mass wasting on conti-  
 50 nental margins. *Annu. Rev. Earth Planet. Sci.*, **16**, 101–119.
- 51 Corzo, A., García de Lomas, J., Van Bergeijk, A., Luzón, A.,  
 52 Mayayo, M.J. and Mata, P. (2005) Carbonate mineralogy  
 53 along a biogeochemical gradient in recent lacustrine sedi-  
 54 ments of Gallocanta Lake (Spain). *Geomicrobiol. J.*, **22**, 1–16.
- 55 Cvijic, J. (1981) The dolines: translation of geography. In: *Karst*  
*Geomorphology* (Ed. ?????), pp. 225–276. Hutchinson,  
 Pennsylvania.
- Dean, W.E. (1981) Carbonate minerals and organic matter in  
 sediments of modern north-temperate hard-water lakes. in:  
*Recent and Ancient Nonmarine Depositional Environments:*  
*Models for Exploration* (Eds E.G. Ethridge and R.M. Flores),  
*SEPM Spec. Publ.*, **31**, 213–231.
- Dean, W.E. and Fouch, T.D. (1983) Lacustrine environment.  
 In: *Carbonate Depositional Environments* (Eds R.A. Scholle,  
 D.G. Bebout and C.H. Moore), *AAPG Mem.*, **33**, 96–130.
- Domínguez-Castro, F., Santisteban, J.I., Mediavilla, R., Dean,  
 W.E., López-Pamo, E., Gil-García, M.J. and Ruiz-Zapata,  
 M.B. (2006) Environmental and geochemical record of hu-  
 man-induced changes in C storage during the last millen-  
 nium in a temperate wetland (Las Tablas de Daimiel  
 National Park, central Spain). *Tellus B*, **58**, 573–585.
- Esteve, I., Guerrero, R., Montesinos, E. and Abellà, C. (1983)  
 Electron microscope study of the interaction of epibiontic  
 bacteria with *Chromatium minus* in natural habitats.  
*Microbial Ecol.*, **9**, 57–64.
- Eugster, H.P. and Hardie, L.A. (1978) Saline lakes. In: *Lakes,*  
*Chemistry, Geology, Physics* (Ed. A. Lerman), pp. 237–293.  
 Springer, New York.
- Eugster, H.P. and Kelts, K.R. (1983) Lacustrine chemical  
 sediments. In: *Chemical Sediments and Geomorphology*  
 (Eds A.S. Goudie and K. Pye), pp. 321–368. Academic Press,  
 London.
- Fritz, S.C., Baker, P.A., Seltzer, G.O., Ballantyne, A., Tapia,  
 P., Cheng, H. and Edwards, R.L. (2007) Quaternary glacia-  
 tion and hydrologic variation in the South American tropics  
 as reconstructed from the Lake Titicaca drilling project.  
*Quatern. Res.*, **68**, 410–420.
- Gierlowski-Kordesch, E.H. and Kelts, K.R. (1994) *Global*  
*Geological Record of Lake Basins*. Cambridge University  
 Press, Cambridge, 427 pp.
- Gierlowski-Kordesch, E.H. and Kelts, K.R. (2000) *Lake Basins*  
 14 *Through Space and Time*. ????????, Tulsa, OK, 648 pp.
- Girardclos, S., Schmidt, O.T., Sturm, M., Ariztegui, D., Pugin,  
 A. and Anselmetti, F.S. (2007) The 1996 AD delta collapse  
 and large turbidite in Lake Brienz. *Mar. Geol.*, **241**, 137–154.
- Guerrero, R., Pedrós-Alió, C., Esteve, I. and Mas, J. (1987)  
 Communities of phototrophic sulfur bacteria in lakes of the  
 Spanish Mediterranean region. *Acta Academiae Aboensis*,  
 15 **2**, 125–151.
- Gutiérrez, F., Calaforra, J., Cardona, F., Ortí, F., Durán, J. and  
 Garay, P. (2008) Geological and environmental implications  
 of the evaporite karst in Spain. *Environ. Geol.*, **53**, 951–965.
- Gutiérrez-Elorza, M. (2001) *Geomorfología Climática*. Editori-  
 al Omega, Barcelona, 642 pp.
- Gutierrez-Santolalla, F., Acosta, E., Rios, S., Guerrero, J. and  
 Lucha, P. (2005) Geomorphology and geochronology of  
 sackung features (uphill-facing scarps) in the Central  
 Spanish Pyrenees. *Geomorphology*, **69**, 298–314.
- Hampton, M.A., Lee, H.J. and Locat, J. (1996) Submarine  
 landslides. *Rev. Geophys.* **34**, 33–59.
- Hardie, L.A., Smoot, J.P. and Eugster, H.P. (1978) Saline lakes  
 and their deposits: a sedimentological approach. In: *Modern*  
*and Ancient Lake Sediments* (Eds A. Matter and M.E.  
 Tucker), *Int. Assoc. Sedimentol. Spec. Publ.*, **2**, 7–42.
- Heegaard, E., Birks, H.J.B. and Telford, R.J. (2005) Relation-  
 ships between calibrated ages and depth in stratigraphical  
 sequences: an estimation procedure by mixed-effect regres-  
 sion. *Holocene*, **15**, 612–618.
- Hodell, D.A., Anselmetti, F.S., Ariztegui, D., Brenner, M.,  
 Curtis, J.H., Gilli, A., Grzesik, D.A., Guilderson, T.J., Müller,  
 A.D., Bush, M.B., Correa-Metrio, A., Escobar, J. and Kutler-  
 olf, S. (2008) An 85-ka record of climate change in lowland  
 Central America. *Quatern. Sci. Rev.*, **27**, 1152–1165.
- IGME (1982) *Mapa Geológico de España 1:50000 No. 289.*  
 Benabarre. Instituto Geológico y Minero de España, Madrid.

- Jopling, A.V. (1975) Early studies on stratified drift. In: *Glaciofluvial and Glaciolacustrine Sedimentation* (Eds A.V. Jopling and B.C. McDonald), *SEPM Spec. Publ.*, **23**, 4–21.
- Julià, R. (1980) *La conca lacustre de banyoles*. Centro d'Estudis Comarcals de Banyoles, Besalu, 188 pp.
- Kazanci, N., Girgin, S. and Dügél, M. (2004) On the limnology of Salda Lake, a large and deep soda lake in southwestern Turkey: future management proposals. *Aquat. Conserv. Mar. Freshwat. Ecosyst.*, **14**, 151–162.
- Kelts, K. and Hsü, K.J. (1978) Freshwater carbonate sedimentation. In: *Lakes: Chemistry, Geology and Physics* (Ed. A. Lerman), pp. 295–323. Springer-Verlag, New York.
- Kindinger, J.L., Davis, J.B. and Flocks, J.G. (1999) Geology and evolution of lakes in north-central Florida. *Environ. Geol.*, **38**, 301–321.
- Lambiase, J. (1990) A model for tectonic control of lacustrine stratigraphic sequences in continental rift basins. In: *Lacustrine Basin Exploration: Case Studies and Modern Analogues* (Ed. B.J. Katz), *AAPG Mem.*, **50**, 265–276.
- Last, W.M. (1990) Paleochemistry and paleohydrology of Ceylon Lake, a salt-dominated playa basin in the northern Great Plains, Canada. *J. Paleolimnol.*, **4**, 219–238.
- Last, W.M. and Vance, R.E. (1997) Bedding characteristics of Holocene sediments from salt lakes of the northern Great Plains, Western Canada. *J. Paleolimnol.*, **17**, 297–318.
- León-Llamazares, A. (1991) *Caracterización agroclimática de la provincia de Huesca (Mapa)*. ?????, Madrid.
- López-Vicente, M. (2007) *Erosión y redistribución del suelo en agroecosistemas mediterráneos: Modelización predictiva mediante SIG y validación con 137Cs (Cuenca de Estaña, Pirineo Central)*. Tesis doctoral, Universidad de Zaragoza, Zaragoza, 212 pp.
- López-Vicente, M., Navas, A. and Machín, J. (2008) Identifying erosive periods by using RUSLE factors in mountain fields of the Central Spanish Pyrenees. *Hydrol. Earth Syst. Sci.*, **12**, 523–535.
- Magny, M., de Beaulieu, J.-L., Drescher-Schneider, R., Vannière, B., Walter-Simonnet, A.-V., Millet, L., Bossuet, G. and Peyron, O. (2006) Climatic oscillations in central Italy during the Last Glacial-Holocene transition: the record from Lake Accesa. *J. Quatern. Sci.*, **21**, 311–320.
- Magny, M., de Beaulieu, J.-L., Drescher-Schneider, R., Vannière, B., Walter-Simonnet, A.-V., Miras, Y., Millet, L., Bossuet, G., Peyron, O., Brugiapaglia, E. and Leroux, A. (2007) Holocene climate changes in the central Mediterranean as recorded by lake-level fluctuations at Lake Accesa (Tuscany, Italy). *Quatern. Sci. Rev.*, **26**, 1736–1758.
- Martin, J. (1981) *Le Moyen Atlas centrale: étude géomorphologique*. Editions du Service Géologique, ?????.
- Martínez-Peña, M.B. and Pocoví, A. (1984) Significado tectónico del peculiar relieve del Sinclinal de Estopiñán (Prepirineo de Huesca). In: *I Congreso Español de Geología, III* (Ed. ???, ?????), pp. 199–206, Segovia, Spain.
- Martín-Puertas, C., Valero-Garcés, B.L., Mata, M.P., González-Sampériz, P., Bao, R., Moreno, A. and Stefanova, V. (2008) Arid and humid phases in Southern Spain during the last 4000 years: The Zoñar Lake Record, Córdoba. *Holocene*, doi: 10.1177/0959683608093533.
- Meyers, P.A. (1997) Organic geochemical proxies of paleoceanographic, paleolimnologic and paleoclimatic processes. *Org. Geochem.*, **97**, 213–250.
- Meyers, P.A. and Lallier-Vergès, E. (1999) Lacustrine sedimentary organic matter records of Late Quaternary paleoclimates. *J. Paleolimnol.*, **21**, 345–372.
- Millet, L., Vannière, B., Verneaux, V., Magny, M., Disnar, J., Laggoun-Défarge, F., Walter-Simonnet, A., Bossuet, G., Ortu, E. and de Beaulieu, J.-L. (2007) Response of littoral chironomid communities and organic matter to late glacial lake-level, vegetation and climate changes at Lago dell'Accesa (Tuscany, Italy). *J. Paleolimnol.*, **38**, 525–539.
- Miracle, M.R. and Gonzalvo, I. (1979) Els llacs càrstics. *Quaderns d'Ecologia Aplicada* **4**, 37–50.
- Mir-Puyuelo, J. (1997) *El Ciclo biogeoquímico del azufre en ecosistemas estratificados. Papel de los compuestos de azufre inorgánico*. Tesis doctoral, Universitat Autònoma de Barcelona, Barcelona.
- Mitchum, R.M., Vail, P.R. and Sangree, J.B. (1977) Seismic stratigraphy and global changes of sea level, part 6: stratigraphic interpretation of seismic reflection patterns in depositional sequences. In: *Seismic Stratigraphy – Applications to Hydrocarbon Exploration* (Ed. C.E. Payton), *AAPG Mem.*, **26**, 117–133.
- Modamio, X., Pérez, V. and Samarra, F. (1988) Lirnnologia del lago de Montcortés (ciclo 1978-79) (Pallars Jussà, Lleida). *Oecologia aquatica*, **9**, 9–17.
- Morellón, M., Valero-Garcés, B., Moreno, A., Gonzalez-Samperiz, P., Mata, P., Romero, O., Maestro, M. and Navas, A. (2008) Holocene palaeohydrology and climate variability in Northeastern Spain: the sedimentary record of Lake Estanya (Pre-Pyrenean range). *Quatern. Int.*, **181**, 15–31.
- Moreno, A., Valero-Garcés, B., González-Sampériz, P. and Rico, M. (2008) Flood response to rainfall variability during the last 2000 years inferred from the Taravilla Lake record (Central Iberian Range, Spain). *J. Paleolimnol.*, **40**, 943–961.
- Murphy, D.H. and Wilkinson, B.H. (1980) Carbonate deposition and facies distribution in a central Michigan marl lake. *Sedimentology*, **27**, 123–135.
- Negendank, J.F.W. and Zolitschka, B. (1993) *Paleolimnology of European Maar Lakes*. Springer-Verlag, New York.
- Nelson, C.H., Bacon, C.R., Robinson, S.W., Adam, D.P., Bradbury, J.P., Barber, J.H., Schwartz, D. and Vagenas, G. (1994) The volcanic, sedimentologic and paleolimnologic history of the Crater Lake caldera floor, Oregon: evidence for small caldera evolution. *Geol. Soc. Am. Bull.*, **106**, 684–704.
- Nicod, J. (1999) Phénomènes karstiques et mouvements de terrain récents dans le Dépt. du Var; Risques naturels (Avignon, 1995). pp. 115–130. CTHS, Paris.
- Nisbet, E.G. and Piper, D.J.W. (1998) Giant submarine landslides. *Nature*, **392**, 329–330.
- Olivera, C., Riera, A., Lambert, J., Banda, E. and Alexandre, P.S.G.d.C. (1994) *Els terratrèmols de l'any 1373 al Pirineu*. Effectes a Espanya i França, ?????, 407 pp.
- Olivera, C., Redondo, E., Lambert, J., Riera Melis, A. and Roca, A. (2006) *Els terratrèmols dels segles XIV i XV a Catalunya*. ?????, ?????, 407 pp.
- Ordóñez, S., Gonzalez Martin, J.A., Garcia del Cura, M.A. and Pedley, H.M. (2005) Temperate and semi-arid tufas in the Pleistocene to Recent fluvial barrage system in the Mediterranean area: The Ruidera Lakes Natural Park (Central Spain). *Geomorphology*, **69**, 332–350.
- Palmquist, R. (1979) Geologic controls on doline characteristics in mantled karst. *Z. fuer Geomorphol. Suppl Bd*, **32**, 90–106.
- Pérez, A., Luzón, A., Roc, A.C., Soria, A.R., Mayayo, M.J. and Sánchez, J.A. (2002) Sedimentary facies distribution and genesis of a recent carbonate-rich saline lake: Gallocanta Lake, Iberian Chain, NE Spain. *Sed. Geol.*, **148**, 185–202.
- Perez-Obiol, R. and Julià, R. (1994) Climatic change on the Iberian Peninsula recorded in a 30 000-yr pollen record from Lake Banyoles. *Quatern. Res.*, **41**, 91–98.

- 1 **Platt, N.H. and Wright, V.T.** (1991) Lacustrine carbonates: facies models, facies distribution and hydrocarbon aspects. In: *Lacustrine Facies Analysis* (Eds P. Anadón, L. Cabrera and K. Kelts), *Int. Assoc. Sedimentol. Spec. Publ.*, **13**, 57–74.
- 2
- 3 **Pulido-Bosch, A.** (1989) Les gypses triasiques de Fuente Camacho. In: *Réunion franco-espagnole sur les karsts d'Andalousie*, (Ed. ???, ?????), pp. 65–82. ?????, ?????.
- 4
- 5 **23** **Ramírez-Moreno, S.** (2003) *Técnicas de biología molecular aplicadas a l'estudi de sistemes estratificats*. Tesis doctoral, Universitat Autònoma de Barcelona, Bellaterra, Spain, 187 pp.
- 6
- 7 **Reed, J.M.** (1998) Diatom preservation in the recent sediment record of Spanish saline lakes: implications for palaeoclimate study. *J. Paleolimnol.*, **19**, 129–137.
- 8
- 9 **Renault, R.W. and Last, W.M.** (1994) *Sedimentology and Geochemistry of Modern and Ancient Saline Lakes*. ?????, Tulsa.
- 10
- 11 **24** **Riera, S., Wansard, R. and Julià, R.** (2004) 2000-year environmental history of a karstic lake in the Mediterranean Pyrenees: the Estanya lakes (Spain). *Catena*, **55**, 293–324.
- 12
- 13 **Riera, S., Lopez-Saez, J.A. and Julia, R.** (2006) Lake responses to historical land use changes in northern Spain: the contribution of non-pollen palynomorphs in a multiproxy study. *Rev. Palaeobot. Palynol.*, **141**, 127–137.
- 14
- 15 **Rodó, X., Giralt, S., Burjachs, F., Comín, F.A., Tenorio, R.G. and Julià, R.** (2002) High-resolution saline lake sediments as enhanced tools for relating proxy paleolake records to recent climatic data series. *Sed. Geol.*, **148**, 203–220.
- 16
- 17 **Romero, L., Camacho, A., Vicente, E. and Miracle, M.** (2006) Sedimentation patterns of photosynthetic bacteria based on pigment markers in Meromictic Lake La Cruz (Spain): paleolimnological implications. *J. Paleolimnol.*, **35**, 167–177.
- 18
- 19 **Romero-Viana, L., Julià, R., Camacho, A., Vicente, E. and Miracle, M.** (2008) Climate signal in varve thickness: Lake La Cruz (Spain), a case study. *J. Paleolimnol.* ???, ???.
- 20
- 21 **25** **Sadori, L. and Narcisi, B.** (2001) The Postglacial record of environmental history from Lago di Pergusa, Sicily. *Holocene*, **11**, 655–671.
- 22
- 23 **Sancho-Marcén, C.** (1988) El Polje de Saganta (Sierras Exteriores pirenaicas, prov. de Huesca). *Cuaternario y Geomorfología*, **2**, 107–113.
- 24
- 25 **26** **Schilts, W.W. and Clague, J.J.** (1992) Documentation of earthquake-induced disturbance of lake sediments using sub-bottom acoustic profiling. *Can. J. Earth Sci.*, **29**, 1018–1042.
- 26
- 27 **Schmidt, R., Müller, J., Drescher-Schneider, R., Krisai, R., Szeroczyńska, K. and Baric, A.** (2000) Changes in lake level and trophy at Lake Vrana, a large karstic lake on the Island of Cres (Croatia), with respect to palaeoclimate and anthropogenic impacts during the last approx. 16 000 years. *J. Limnol.*, **59**, 113–130.
- 28
- 29 **Schnellmann, M., Anselmetti, F.S., Giardini, D. and McKenzie, J.A.** (2005) Mass movement-induced fold-and-thrust belt structures in unconsolidated sediments in Lake Lucerne (Switzerland). *Sedimentology*, **52**, 271–289.
- 30
- 31 **Schnurrenberger, D., Russell, J. and Kelts, K.** (2003) Classification of lacustrine sediments based on sedimentary components. *J. Paleolimnol.*, **29**, 141–154.
- 32
- 33 **Schreiber, B.C. and Tabakh, M.E.** (2000) Deposition and early alteration of evaporites. *Sedimentology*, **47**, 215–238.
- 34
- 35 **Shaw, B., Klessig, L. and Mechenich, C.** (2002) *Understanding Lake Data*. University of Wisconsin Cooperative Extension, ?????.
- 36
- 37 **27** **Smoot, J.P. and Lowenstein, T.** (1991) Depositional environments of non-marine evaporites. In: *Evaporites, Petroleum and Mineral Resources* (Ed. J. Melvin), *Dev. Sedimentol.*, **50**, 189–348. Elsevier, Amsterdam.
- 38
- 39 **Strasser, M., Stegmann, S., Bussmann, F., Anselmetti, F.S., Rick, B. and Kopf, A.** (2007) Quantifying subaqueous slope stability during seismic shaking: Lake Lucerne as model for ocean margins. *Mar. Geol.*, **240**, 77–97.
- 40
- 41 **Street-Perrott, F.A. and Harrison, S.P.** (1985) Lake levels and climate reconstruction. In: *Paleoclimate Analysis and Modeling* (Ed. A. Hecht), pp. 291–340. Wiley, New York.
- 42
- 43 **Talbot, M.R. and Allen, P.A.** (1996) Lakes. In: *Sedimentary Environments: Processes, Facies and Stratigraphy* (Ed. H.G. Reading), pp. 83–124. Blackwell Science, Oxford.
- 44
- 45 **Valero Garcés, B.L., Moreno, A., Navas, A., Mata, P., Machín, J., Delgado Huertas, A., Gonzalez Samperiz, P., Schwalb, A., Morellon, M., Cheng, H. and Edwards, R.L.** (2008) The Taravilla lake and tufa deposits (Central Iberian Range, Spain) as palaeohydrological and palaeoclimatic indicators. *Palaeogeogr. Palaeoclimatol. Palaeoecol.*, **259**, 136–156.
- 46
- 47 **Valero-Garcés, B.L. and Kelts, K.R.** (1995) A sedimentary facies model for perennial and meromictic saline lakes: Holocene Medicine Lake Basin, South Dakota, USA. *J. Paleolimnol.*, **14**, 123–149.
- 48
- 49 **Valero-Garcés, B., Navas, A., Machín, J., Stevenson, T. and Davis, B.** (2000) Responses of a saline Lake Ecosystem in a semiarid region to irrigation and climate variability: the history of Salada Chiprana, Central Ebro Basin, Spain. *Ambio*, **29**, 344–350.
- 50
- 51 **Valero-Garcés, B., Navas, A., Mata, P., Delgado-Huertas, A., Machín, J., González-Sampérez, P., Moreno, A., Schwalb, A., Ariztegui, D., Schnellmann, M., Bao, R. and González-Barrios, A.** (2003) Sedimentary facies analyses in lacustrine cores: from initial core descriptions to detailed palaeoenvironmental reconstructions. A case study from Zoñar Lake (Cordoba province, Spain). In: *Limnogeology in Spain: A Tribute to Kerry Kelts* (Ed. B. Valero-Garcés), *Bibl. Cienc.*, ?????, 385–414. C.S.I.C., Madrid.
- 52
- 53 **28** **Valero-Garcés, B., González-Sampérez, P., Navas, A., Machín, J., Delgado-Huertas, A., Peña-Monné, J.L., Sancho-Marcén, C., Stevenson, T. and Davis, B.** (2004) Palaeohydrological fluctuations and steppe vegetation during the Last Glacial Maximum in the central Ebro valley (NE Spain). *Quatern. Int.*, **122**, 43–55.
- 54
- 55 **Valero-Garcés, B., González-Sampérez, P., Navas, A., Machín, J., Mata, P., Delgado-Huertas, A., Bao, R., Moreno, A., Carrión, J.S., Schwalb, A. and González-Barrios, A.** (2006) Human impact since medieval times and recent ecological restoration in a Mediterranean lake: the Laguna Zoñar, southern Spain. *J. Paleolimnol.*, **35**, 441–465.
- Villa, I. and Gracia, M.L.** (2004). *Estudio hidrogeológico del sinclinal de Estopiñán (Huesca)*. XXXVIII CHIS. Confederación Hidrográfica del Ebro, ?????.
- 29** **Wansard, G., De Deckker, P. and Julia, R.** (1998) Variability in ostracod partition coefficients D(Sr) and D(Mg): implications for lacustrine palaeoenvironmental reconstructions. *Chem. Geol.*, **146**, 39–54.
- Wright, V.P.** (1990) Lacustrine carbonates. In: *Carbonate Sedimentology* (Ed. M.E. Tucker and V.P. Wright), pp. 164–190. Blackwell Scientific Publications, Oxford.
- Zanchetta, G., Borghini, A., Fallick, A., Bonadonna, F. and Leone, G.** (2007) Late Quaternary palaeohydrology of Lake Pergusa (Sicily, southern Italy) as inferred by stable isotopes of lacustrine carbonates. *J. Paleolimnol.*, **38**, 227–239.

Manuscript received 11 April 2008; revision accepted 13 November 2008



# Author Query Form

Journal: SED

Article: 1044

Dear Author,

During the copy-editing of your paper, the following queries arose. Please respond to these by marking up your proofs with the necessary changes/additions. Please write your answers on the query sheet if there is insufficient space on the page proofs. Please write clearly and follow the conventions shown on the attached corrections sheet. If returning the proof by fax do not write too close to the paper's edge. Please remember that illegible mark-ups may delay publication.

Many thanks for your assistance.

| Query reference | Query  | Remarks |
|-----------------|--|---------|
| 1               | <b>AUTHOR: Please supply a short title that will be used as the running head.</b>  |         |
| 2               | <b>AUTHOR: The unit for electrical conductivity has been changed from 'μS' to 'μS cm<sup>-1</sup>'. Please check.</b>                                    |         |
| 3               | <b>AUTHOR: Please define TDS.</b>  |         |
| 4               | <b>AUTHOR: Please give manufacturer information for KINGDOM SUITE software: company name, town, state (if USA), and country.</b>                         |         |
| 5               | <b>AUTHOR: Please give manufacturer information for ARCMAP 9.0®: company name, town, state (if USA), and country.</b>                                    |         |
| 6               | <b>AUTHOR: Please give city name for Poznan Radiocarbon Laboratory.</b>  |         |
| 7               | <b>AUTHOR: Reimer <i>et al.</i>, 2004 has been changed to Riera <i>et al.</i>, 2004 so that this citation matches the list.</b>                          |         |
| 8               | <b>AUTHOR: Please provide the name of the publisher for Reference Alagöz (1967).</b>   |         |
| 9               | <b>AUTHOR: Please confirm that Journal title Oecologia Aquatica has been abbreviated correctly.</b>  |         |
| 10              | <b>AUTHOR: Please check volume number in reference Bauld (1981).</b>   |         |
| 11              | <b>AUTHOR: Bradley <i>et al.</i> (2003) has not been cited in the text. Please indicate where it should be cited; or delete from the Reference List.</b> |         |
| 12              | <b>AUTHOR: Please provide the page range for this chapter in Reference Buurman <i>et al.</i> (1997).</b>   |         |
| 13              | <b>AUTHOR: Please supply editor name in reference Cvijic (1981).</b>   |         |
| 14              | <b>AUTHOR: Please provide the name of the publisher for Reference Gierlowski-Kordesch <i>et al.</i> (2000).</b>  |         |

|    |  |  |
|----|--|--|
| 15 | AUTHOR: Please confirm that Journal title Acta Academiae Aboensis has been abbreviated correctly.                              |  |
| 16 | AUTHOR: Please provide the name of the publisher for Reference León-Llamazares (1991).   |  |
| 17 | AUTHOR: Please provide the city location of publisher for Reference Martin (1981).   |  |
| 18 | AUTHOR: Please provide the Editors for Reference Martínez-Peña and Pocoví (1984).  |  |
| 19 | AUTHOR: Please provide volume number and page range in reference Martín-Puertas et al. (2008) if now published.                |  |
| 20 | AUTHOR: Please confirm that Journal title Quaderns d'Ecologia Aplicada has been abbreviated correctly.                         |  |
| 21 | AUTHOR: Please provide the city location of publisher for Reference Olivera et al. (1994).                                     |  |
| 22 | AUTHOR: Please provide name and city location of publisher for Reference Olivera et al. (2006).                                |  |
| 23 | AUTHOR: Please provide editor name(s), city location and name of publisher for Reference Pulido-Bosch (1989).                  |  |
| 24 | AUTHOR: Please provide the name of the publisher for Reference Renault and Last (1994).  |  |
| 25 | AUTHOR: Please update reference Romero-Viana et al. (2008) with volume number and page range.                                  |  |
| 26 | AUTHOR: Please confirm that Journal title Cuaternario y Geomorfología has been abbreviated correctly.                          |  |
| 27 | AUTHOR: Please provide the city location of publisher for Reference Shaw et al. (2002).  |  |
| 28 | AUTHOR: Please provide volume number in reference Valero-Garcés et al. (2003).   |  |
| 29 | AUTHOR: Please provide the city location of publisher for Reference Villa and Gracia (2004).                                   |  |
| 30 | AUTHOR: <i>Ávila et al.</i> , 1982 has been changed to <i>Ávila et al.</i> , 1984 so that this citation matches the list.      |  |
| 31 | AUTHOR: <i>Heegard et al.</i> , 2005 has been changed to <i>Heegaard et al.</i> , 2005 so that this citation matches the list. |  |

# MARKED PROOF

## Please correct and return this set

Please use the proof correction marks shown below for all alterations and corrections. If you wish to return your proof by fax you should ensure that all amendments are written clearly in dark ink and are made well within the page margins.

| <i>Instruction to printer</i>                                  | <i>Textual mark</i>   | <i>Marginal mark</i>                          |
|--|---|---|
| Leave unchanged  | ... under matter to remain  | Ⓟ   |
| Insert in text the matter indicated in the margin              | ∧   | New matter followed by<br>∧ or ∧ <sup>Ⓢ</sup> |
| Delete   | / through single character, rule or underline<br>or<br>┌───┐ through all characters to be deleted | Ⓞ or Ⓞ <sup>Ⓢ</sup>                           |
| Substitute character or substitute part of one or more word(s) | / through letter or<br>┌───┐ through characters   | new character / or<br>new characters /        |
| Change to italics  | — under matter to be changed  | ↙   |
| Change to capitals   | ≡ under matter to be changed  | ≡   |
| Change to small capitals                                       | ≡ under matter to be changed  | ≡   |
| Change to bold type  | ~ under matter to be changed  | ~   |
| Change to bold italic  | ≈ under matter to be changed  | ≈   |
| Change to lower case   | Encircle matter to be changed   | ≡   |
| Change italic to upright type                                  | (As above)  | ⊕   |
| Change bold to non-bold type                                   | (As above)  | ⊖   |
| Insert 'superior' character                                    | / through character or<br>∧ where required  | Υ or Υ<br>under character<br>e.g. Υ or Υ      |
| Insert 'inferior' character                                    | (As above)  | ∧<br>over character<br>e.g. ∧                 |
| Insert full stop   | (As above)  | ⊙   |
| Insert comma   | (As above)  | ,   |
| Insert single quotation marks                                  | (As above)  | Ƴ or ƴ and/or<br>ƶ or Ʒ                       |
| Insert double quotation marks                                  | (As above)  | ƶ or Ʒ and/or<br>Ʒ or ƶ                       |
| Insert hyphen  | (As above)  | ⊥   |
| Start new paragraph  | ┌   | ┌   |
| No new paragraph   | ┐   | ┐   |
| Transpose  | └┐  | └┐  |
| Close up   | linking ○ characters  | Ⓞ   |
| Insert or substitute space between characters or words         | / through character or<br>∧ where required  | Υ   |
| Reduce space between characters or words                       |   | ↑   |